

Acidification, deoxygenation, nutrient and biomasses decline in a warming Mediterranean Sea

Marco Reale¹, Gianpiero Cossarini¹, Paolo Lazzari¹, Tomas Lovato², Giorgio Bolzon¹, Simona Masina², Cosimo Solidoro¹, Stefano Salon¹

1. National Institute of Oceanography and Applied Geophysics - OGS, Trieste, Italy

2. Fondazione Centro euro-Mediterraneo sui Cambiamenti Climatici, CMCC, Ocean Modeling and Data Assimilation Division, Bologna, Italy

Correspondence to: Marco Reale (mreale@inogs.it) and Stefano Salon (ssalon@inogs.it)

Abstract. The projected warming, nutrient decline, changes in net primary production, deoxygenation and acidification of the global ocean will ~~dramatically likely~~ affect marine ecosystems during the 21st century. ~~Here we assess the~~ Here the climate change-related impacts in the marine ecosystems of the Mediterranean Sea in the middle and at the end of the 21st century are assessed using high-resolution projections of the physical and biogeochemical state of the basin under the Representative Concentration Pathways (RCPs) 4.5 and 8.5. The analysis shows in shows in both scenarios significant changes in the dissolved nutrient content of the euphotic and intermediate layers of the basin, of the net primary production, and phytoplankton respiration and carbon stock (including phytoplankton, zooplankton, bacterial biomass and particulate organic matter). ~~The analysis shows significant changes in the dissolved nutrient content of the euphotic and intermediate layers of the basin, net primary production, phytoplankton respiration and carbon stock (including phytoplankton, zooplankton, bacterial biomass and particulate organic matter).~~ The projections also show an uniform surface and subsurface reduction in the oxygen concentration driven by the warming of the water column and by the increase in ecosystem respiration, and. ~~Moreover, we observe~~ an acidification signal was observed in the upper water column, linked to the increase in the dissolved inorganic carbon content of the water column due to CO₂ absorption from the atmosphere and the increase in respiration. The projected changes are stronger in the RCP8.5 (worst-case) scenario and, in particular, in the Eastern Mediterranean due to the limited influence of the exchanges in the Strait of Gibraltar in that part of the basin. On the other hand, the analysis of the projections under RCP4.5 emission scenario shows a tendency to recover the values observed at the beginning of the 21st century for several biogeochemical variables in the second half of the period. This result supports the idea - possibly based on the existence, in a system like the Mediterranean Sea, of a certain buffer capacity and renewal rate - that the implementation of policies of reducing CO₂ emission could be, indeed, effective and could contribute to the foundation of ocean sustainability science and policies. ~~The projected changes are stronger in the eastern Mediterranean due to the limited influence, in that part of the basin, of the exchanges in the Strait of Gibraltar.~~

1. Introduction

The Mediterranean Sea (Fig. 1) is a mid-latitude semi-enclosed basin surrounded by the continental areas of Southern Europe, Northern Africa and the Middle East. The basin is characterized by a thermohaline circulation composed of three distinctive cells. The first is an open cell associated with the inflow of the Atlantic Water (AW) at the Strait of Gibraltar (which undergoes a progressive increase in salinity due to evaporation becoming Modified Atlantic Water, or MAW) and the formation of Levantine Intermediate Water (LIW) in the Eastern basin (Lascaratos, 1993; Nittis and Lascaratos, 1998; Velaoras et al., 2019; Fach et al., 2021; Fedele et al., 2021; Lascaratos, 1993; Nittis and Lascaratos, 1998). The other two are closed cells associated with deep water formation processes occurring in the Gulf of Lions (located in the North Western Mediterranean, Fig.1; Somot et al., 2018 and reference therein) and in the Adriatic Sea (Fig. 1; Mantziafou and Lascaratos 2004, 2008; Schroeder et al., 2012 and references therein).

Future climate projections for the Mediterranean region based on different emission scenarios show, at the end of the 21st century, (i) a reduction in precipitation and a general warming of the area (e.g., Giorgi, 2006; Diffenbaugh et al., 2007; Giorgi and Lionello, 2008; Dubois et al., 2012; Lionello et al., 2012; Planton et al., 2012; Gualdi et al., 2013; MedEEC, 2020), (ii) a warming of seawater (Somot et al., 2006; Adloff et al., 2015; Soto-Navarro et al., 2020; MedECC, 2020), and (iii) a consistent weakening of the thermohaline circulation and an increase in the stratification index throughout the basin (Somot et al., 2006; Adloff et al., 2015; Soto-Navarro et al., 2020) and a further increase in frequency and severity of atmospheric and marine heat waves and drought (Galli et al., 2017; Darmaraki et al., 2019; Ibrahim et al., 2021; Mathbout et al., 2021). Conversely, the future evolution of sea surface salinity in the Mediterranean Sea and the sign of its change are still uncertain due to the role played by rivers and Strait of Gibraltar exchanges (Adloff et al., 2015; Soto-Navarro et al., 2020; MedECC, 2020). In general, the magnitude of the projected changes has been shown to be dependent on the adopted emission scenario (MedECC,2020).

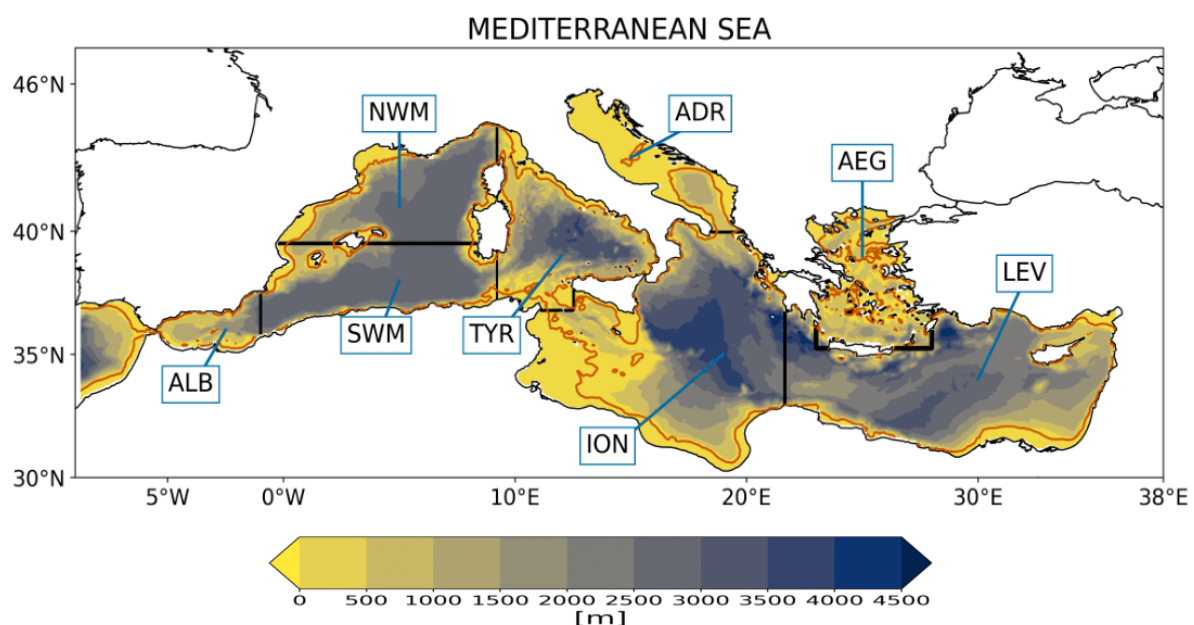


Fig.1 Mediterranean Sea bathymetry (in m); the Atlantic buffer zone and relative sub-basins considered in the analysis: Albanian Sea (ALB), North Western Mediterranean (NWM), South Western Mediterranean (SWM), Tyrrhenian (TYR), Adriatic Sea (ADR), Ionian Sea (ION), Aegean Sea (AEG), Levantine basin (LEV). The dark orange line

marks the 200m isobath in the model domain. ~~The domain boundary is set at longitude 8.8°W, area-westward of outside the Strait of Gibraltar~~ Gibraltar strait is the buffer zone of the computational domain where boundary conditions are applied.

From a biogeochemical point of view, the Mediterranean Sea is considered as an oligotrophic (ultraoligotrophic in its ~~eastern~~ Eastern part) basin (Bethoux et al., 1998; Moutin and Raimbault, 2002; Siokou-Frangou et al., 2010; Lazzari et al., 2012). It is characterized by low productivity levels and an east-west trophic gradient (Crise et al., 1999; D'Ortenzio and Ribera d'Alcala 2009; Lazzari et al., 2012) which results from the superposition of different mechanisms such as the biological pump, the estuarine inverse circulation, and the position of nitrate (NO₃) and phosphate (PO₄) sources (Crise et al., 1999; Crispi et al., 2001). The only exceptions to the oligotrophy of the basin are some areas (Gulf of Lions, Strait of Sicily, Algerian coastlines, Southern Adriatic Sea, Ionian Sea, Aegean Sea and Rhodes Gyre) where strong vertical mixing and upwelling phenomena associated with air-sea interactions and wind stress forcing enrich the surface in nutrients, so favouring phytoplankton rapid growth (or bloom) mostly in the late winter-early spring period (D'Ortenzio and Ribera d'Alcala, 2009; Reale et al., 2020b). A proxy widely adopted to detect phytoplankton blooms is the surface concentration of chlorophyll-*a* that is characterized by relative high values in specific open sea/coastal areas, where it is linked to the physical forcing and river inflow (D'Ortenzio and Ribera d'Alcala, 2009; Lazzari et al., 2012; Herrmann et al., 2013; Auger et al., 2014; Richon et al., 2018; Di Biagio et al., 2019; Reale et al., 2020a). The open sea chlorophyll-*a* vertical dynamics follows a seasonal cycle with winter-early spring surface blooms, and summer onset of a deep chlorophyll-*a* maximum (DCM) which deepens from approximately 50 m in the ~~western~~ Western areas to 100 m in the ~~eastern~~ Eastern areas (e.g. Lazzari et al., 2012; Macias et al., 2014; Lavigne et al., 2015; Cossarini et al., 2021).

Due to the strong links between ocean/atmosphere dynamics and biogeochemical patterns, it has to be expected that future climate change will have relevant impacts on the biogeochemistry and, in turn, on the marine ecosystem dynamics of the Mediterranean Sea. In fact, all the projected ~~physical~~ changes for the region will likely affect the vertical mixing and reduce the nutrient supply into the euphotic layer of the Mediterranean Sea (e.g. Richon et al., 2019), which is essential for phytoplankton dynamics and productivity, with possible impacts on the biogeochemical carbon cycle and CO₂ exchange with the atmosphere (e.g., Lazzari et al., 2012; Cossarini et al., 2015; Canu et al., 2015; Solidoro et al., 2022+).

An assessment of the effects of climate change on the biogeochemistry and marine ecosystem dynamics of the Mediterranean Sea has been considered in a number of previous studies based on different emission scenarios. Hermann et al. (2014) assessed the response of the pelagic planktonic ecosystem of the North-Western Mediterranean to different emission scenarios and showed that, at end of the 21st century, the biogeochemical processes and marine ecosystem components should be very similar to those observed at the end of the 20th century, although quantitative differences might be observed, such as an increase in the bacteria growth, gross primary production and biomass of small-size phytoplankton group might be observed. Lazzari et al. (2014) found a negative change in the plankton biomass in response to the A1B emission scenario climate change, resulting from an increase of productivity and community respiration. Howes et al. (2015) found an increase in the pteropod abundance in the area of the Gulf of Genoa in response to the increase/decrease of sea water temperature/pH in the period 1967-2003. Benedetti et al. (2018), using environmental niche models and considering six physical simulations based on different emission scenarios (A2, A2-F, A2-RF, A2-ARF, A1B-ARF, B1-ARF; Adloff et al., 2015), projected, in response to climate change, a loss of copepods diversity

throughout most of the surface layer of the Mediterranean Sea. On the other hand, Moullec et al. (2019) under RCP8.5 emission scenario found an increase/decrease in both phytoplankton biomass and net primary production by the end of the 21st century in the Eastern/Western Mediterranean Sea. Macias et al. (2015) showed that, under emission scenarios RCP4.5 and RCP8.5 and despite a significant observed warming trend, the mean integrated primary production rate in the entire basin will remain almost unchanged in the 21st century. However, they pointed out some peculiar spatial differences in the basin such as an increase in the oligotrophy of the ~~western~~Western basin due to a surface density decrease and an increase in net primary production in the ~~eastern~~Eastern basin due to the increased density. Richon et al. (2019) observed, under the A2 emission scenario (which is similar to the RCP8.5 emission scenario in terms of magnitude of the projected changes in the global mean temperature), an accumulation of nitrate in the basin and a reduction of 10% in net primary productivity by 2090, with a peak of 50% in specific areas (including the Aegean Sea). On the other hand, no tendencies in the phosphorus were observed. Pagès et al. (2020) showed, under emission scenario RCP8.5, a decline (~~stronger in NO₃ than PO₄~~) in the nutrient concentration (~~stronger in NO₃ than PO₄~~) at the surface of the basin due to the increase in the vertical stratification and pointed out that the Mediterranean Sea will become less productive (14% decrease in integrated primary production in both ~~western~~Western and ~~eastern~~Eastern basins) and will be characterized by a reduction (22% in the ~~western~~Western basin and 38% in the ~~eastern~~Eastern basin) in large phytoplankton species abundance in ~~favor~~favour of small organisms. All these changes will mainly affect the ~~western~~Western basin, while the ~~eastern~~Eastern basin will be less impacted (Pagès et al., 2020). Solidoro et al. (2022⁺) discussed the evolution of the carbon cycling, budgets and fluxes of the basin under the A2 scenario, highlighting an increase in the trophodynamic carbon fluxes and showing, at the same time, that the increment in the plankton primary production will be more than compensated by the increase in the ecosystem total respiration, which corresponds to a decrease of the total living carbon and oxygen in the epipelagic layer. Moreover, Solidoro et al., (2022)the work also projected an increase of dissolved inorganic carbon (DIC) pool and quantified for the first time the related acidification of the basin, a process that might significantly alter the Mediterranean ecosystems (Zunino et al., 2017; 2019) and their capability to ~~sustain~~ provide ecosystem services (Zunino et al., 2021).

All ~~of the above-mentioned~~ these previous works demonstrate that the dynamics of the marine ecosystem may be affected directly and indirectly by climate change ~~and the magnitude of their response is dependent on the emission scenario adopted.~~The Different levels of warming, acidification and changes in the vertical distribution of the oxygen, nutrient concentration and net primary production related to water column stratification are all potential marine stressors affecting marine organisms and ecosystem dynamics (see Kwiatkowski et al., 2020 for a review about the synergistic effects among potential marine stressors).

~~A~~Moreover, a proper simulation of these marine stressors and related impacts require the adoption of suitable horizontal and vertical resolutions. In fact, it has been shown that meso and submesoscale structures of the Mediterranean circulation influence indeed the biogeochemical dynamics of many areas of the basin (Moutin and Prieur, 2012; Richon et al., 2019), while the vertical resolution affects the features of the simulated stratification and subsurface ventilation pathways (see Kwiatkowski et al., 2020 and reference therein for a review).

These considerations emphasize the importance of providing eddy-resolving future projections of the Mediterranean Sea biogeochemistry ~~under different emission scenarios~~ that further extend the analysis of the climate change related impacts

in the marine ecosystems of the basin under different emission scenarios. In fact, although observational and modeling studies have been already carried out in the recent period to assess the importance of the mesoscale dynamics on the physical and biogeochemical state of limited areas of the Mediterranean Sea (e.g. Hermann et al., 2008; Moutin and Prieur, 2012; Guyennon et al., 2015; Ramirez-Romero et al., 2020), ~~These~~ long-term eddy-resolving biogeochemical projections ~~under different emission scenarios~~, to the best of the authors' knowledge, have not been analyzed so far in the region. ~~Such projections and that~~ might be used in future studies specifically focused on the analysis of climate change impact on specific organisms, habitats and/or local areas.

Therefore, here ~~we assess the~~ climate change-related impacts in the marine ecosystems of the Mediterranean Sea in the middle and at the end of the 21st century ~~are assessed~~ using eddy-resolving projections (~~1/16° and 70 vertical levels~~) of the physical and biogeochemical state of the basin under emission scenarios RCP4.5 and RCP8.5. These projections are derived from the offline coupling between the physical model MFS16 (Mediterranean Forecasting System at 1/16°; Oddo et al., 2009) and the transport-reaction model OGSTM-BFM (OGS Transport Model-Biogeochemical Flux Model; Lazzari et al., 2012). ~~The analysis~~ ~~We~~ focuses on 21st century projected changes ~~of~~ dissolved nutrients and oxygen, net primary production, respiration, living/non-living organic matter, plankton and bacterial biomass, and particulate organic matter (POC). Moreover, the response of the basin to the increasing atmospheric CO₂ concentrations is thoroughly investigated. The ~~projected~~ ~~observed~~ changes are also correlated with changes in the physical forcing in the region.

The article is organized as follows: the MFS16-OGSTM-BFM system along with the physical forcing used to drive the biogeochemical scenarios, initial and boundary conditions and numerical experiments are described in Section 2. Section 3 discusses the projected changes in climate change-related impacts in the marine ecosystems of the Mediterranean basin. Finally, Section 4 summarizes and discusses the results of this work, together with their uncertainties, paving the way for possible future research avenues.

1. Data and Methods

The biogeochemical projections of the Mediterranean Sea state during the 21st century have been produced by driving the transport-reaction model OGSTM-BFM (Lazzari et al., 2012) with the 3D outputs of the physical model MFS16 (Oddo et al., 2009) through an off-line coupling. In fact, the physical model MFS16 supplies to the OGSTM-BFM the temporal evolution of daily horizontal and vertical current velocities, vertical eddy diffusivity, potential temperature, salinity, and surface data for solar shortwave irradiance and wind stress. The resulting transport processes affecting the concentration of biogeochemical tracers (advection, vertical diffusion and sinking) are computed by OGSTM, which is a modified version of the OPA tracer model (Océan PArallélisé, Foujols et al., 2000). The temporal evolution of biogeochemical processes is computed by the Biogeochemical Flux Model (BFM; Vichi et al., 2015).

2.1. The MFS16 physical model

MFS16 is the Mediterranean configuration of the NEMO modelling system ([Nucleus for European Modelling of the Ocean](#); Madec, 2008; see also <http://www.nemo-ocean.eu>, version 3.4) and constitutes the climate implementation of the Mediterranean Ocean Forecasting System (Oddo et al., 2009; Lovato et al., 2013).

The ~~original MFS16 model~~ domain covers the whole Mediterranean Sea and part of the neighboring Atlantic Ocean region (~~Fig. 1~~) with a horizontal grid resolution of $1/16^\circ$ (~ 6.5 km) and 72 unevenly spaced vertical levels (ranging from 3 m at the surface down to 600 m in the deeper layers, [see Lovato et al., 2013](#)). The model computes the air-sea fluxes of water, momentum and heat using specific bulk formulae tuned for the Mediterranean Sea (Oddo et al., 2009) applied to the atmospheric fields obtained from the atmosphere-ocean general circulation model CMCC-CM ([CMCC-Coupled model](#); Scoccimarro et al., 2011).

The open boundary conditions in the Atlantic region for the physical variables (zonal/meridional component of current velocity, sea surface height, temperature and salinity) were derived from the ocean component of the CMCC-CM coupled model, while the riverine freshwater discharges and fluxes in the Dardanelles Strait were provided by the hydrological component of the same coupled model (Gualdi et al., 2013). The initial conditions of the Mediterranean Sea were obtained from the gridded temperature and salinity data produced by the SeaDataNet infrastructure (<http://www.seadatanet.org/>). The model was initially spun-up for 25 years under present climate conditions and then scenario simulations were performed over the 2005-2100 period.

2.2. The OGSTM-BFM transport-reaction model

The OGSTM-BFM transport-reaction model is based on the coupling of a transport model (OGSTM) based on the OPA system (Foujols et al., 2000) and the BFM biogeochemical reactor. OGSTM-BFM is fully described in Lazzari et al. (2012, 2016), where it was used to simulate chlorophyll-*a*, primary production and nutrient dynamics of the Mediterranean Sea for the 1998-2004 period.

The OGSTM transport model resolves the advection, vertical diffusion and the sinking terms of the biogeochemical tracers. The temporal scheme of OGSTM is an explicit forward temporal scheme for the advection and horizontal diffusion terms, whereas an implicit time scheme is adopted for the vertical diffusion. The BFM biogeochemical reactor considers co-occurring effects of multi-nutrient interactions and energy/material fluxes through the classical food chain and the microbial food web which are both very important in the Mediterranean Sea (Bethoux et al., 1998). BFM has been extensively applied to the studies of the dynamics of dissolved nutrients, chlorophyll-*a* and net primary production in the Mediterranean Sea (Lazzari et al., 2012; 2016; Di Biagio et al., 2019; Reale et al., 2020a), marine carbon sequestration and alkalinity (Canu et al., 2015; Cossarini et al., 2015; Butenschön et al., 2021), impacts of climate change on the biogeochemical dynamics of marine ecosystems (Lazzari et al., 2014; Lamon et al., 2014; Solidoro et al., 2021), influence of large-scale atmospheric circulation patterns on nutrient dynamics (Reale et al., 2020b) and operational short-term forecasts for the Mediterranean Sea biogeochemistry (Teruzzi et al. 2018; 2019; Salon et al., 2019). The version adopted here is the v5.

The model simulates the biogeochemical cycles of carbon, nitrogen, phosphorus and silicon through dissolved forms and living organic and non-living organic compartments (labile, semi-labile and semi-refractory organic matter). Moreover, it presently includes nine plankton functional types (PFTs), meant to be representative of diatoms, flagellates, picophytoplankton, dinoflagellates, carnivorous and omnivorous mesozooplankton, bacteria, heterotrophic nanoflagellates and microzooplankton. It also simulates the carbonate system dynamics, by solving the set of physico-chemical equilibria related to [total alkalinity \(ALK\)](#) and dissolved inorganic carbon (DIC) chemical reactions (Cossarini et al., 2015). [Total alkalinity](#) variability is driven by processes that alter the ion concentration in seawater (nitrification, denitrification, uptake and release of nitrate, ammonia and phosphate by plankton cells, and precipitation and dissolution of [carbonate calcium](#) (CaCO_3), see Wolf-Gladrow et al., 2007). DIC dynamics are driven by biological processes (photosynthesis and respiration, precipitation and dissolution of CaCO_3) and physical processes (CO_2 exchanges at the air-sea interface and, as for all the other biogeochemical tracers, dilution-concentration due to evaporation minus precipitation processes).

2.3. Initial and boundary conditions for the biogeochemistry

~~The initial conditions for the dissolved oxygen, nutrient, silicate and carbonate system variables are based on Medar-Medatlas dataset, as described in Cossarini et al. (2015) and Salon et al. (2019).~~

Boundary conditions are adopted to represent the external supply of biogeochemical tracers and properties from the Strait of Gibraltar. Gibraltar Strait and the Mediterranean rivers into the Mediterranean basin. The exchanges of nutrients and other biogeochemical tracers in the Strait of Gibraltar are achieved by relaxing the 3D fields in the Atlantic zone (Fig. 1) to average vertical profiles which, for dissolved oxygen, phosphate, nitrate and silicate, refer to Salon et al. (2019), while total alkalinity is based on what was described in Cossarini et al. (2015). These profiles do not consider a seasonal cycle or a future temporal evolution, with DIC as the only exception, which is prescribed from a global ocean-climate simulation under RCP8.5 emission scenario performed within the framework of the CMIP5 project (Coupled Model Intercomparison Project Phase 5; Taylor et al., 2012) and based on the CMCC-CESM modeling system (CMCC-Coupled Earth System Model; Vichi et al., 2011). The reasons for these choices rely on: (i) anomalous values observed in N:P ratio under the RCP8.5 emission scenario, (ii) negligible variation, under emission scenario RCP8.5, of the total alkalinity along the 21st century, (iii) lack of a consistent RCP4.5 scenario, (iv) the possibility, using the same conditions at the Atlantic boundary, to test the impacts of the different atmospheric and ocean forcings. Riverine inputs of phosphate, nitrate, dissolved oxygen, [total alkalinity](#) and DIC are based on the PERSEUS FP7-287600 project dataset ([Policy-oriented marine environmental research in the southern European seas](#); Van Apeldoorn and Bouwman, 2014) and, also in this case, do not include temporal evolution in the future scenarios.

As observed in previous works (e.g. Richon et al., 2019), a transient scenario for the evolution of the atmospheric deposition of nitrogen and phosphorus over the Mediterranean Sea is presently not available. Following Di Biagio et al. (2019) and Reale et al. (2020a), the atmospheric deposition of phosphate and nitrate is parametrized as a mass flux at the surface and is set for the entire basin equal to 4780 Mmol year⁻¹ for phosphate and 81275 Mmol year⁻¹ for nitrate. Additional boundary conditions consider the sequestration of inorganic compounds in the marine sediment at the seabed.

~~Finally,~~ the Representative Common Pathway (RCP) 4.5 and 8.5 emission scenarios (Moss et al., 2010) were used to force the coupled physical-biogeochemical MFS16-OGSTM-BFM system. RCP4.5 represents an intermediate scenario in which CO₂ emissions peak around 2040 (causing the maximum increase in CO₂ concentration), and then decline (with a resulting CO₂ concentration plateau) while the RCP8.5 represents the worst-case scenario, in which CO₂ emissions (eventually driven by feedback effects such as the release of greenhouse gasses from the permafrost) will continue to increase throughout the 21st century, and the pCO₂ concentration will rise to more than 1200 ppm at the end of the 21st century (IPCC, 2014). Recently some authors have begun to consider the RCP8.5 scenario as “implausible”, being based, for example, on a large use of coal, larger than its effective availability at the end of 21st century (e.g. Hausfather and Peters, 2020). On the other hand, it is still widely used to assess in the Mediterranean region the potential risks (also in the marine ecosystems) emerging in an extreme warm world climate (5 oC) with respect to the pre-industrial era (IPCC, 2014). Because of that the projections under this emission scenario are still discussed here.

The initial conditions for the dissolved oxygen, nutrient, silicate and carbonate system variables are based on Medar-Medatlas dataset (Mediterranean Data Archeology and Rescue-Mediterranean Atlas), as described in Cossarini et al. (2015) and Salon et al. (2019).

Finally, all the simulations discussed in the next sections, use as initial conditions the resulting final fields from a run that started in January, 1st 2005 following a spin-up of 100 years made with a loop over the 2005–2014 period for the physical forcing, the river nutrient discharge and atmospheric forcing (nutrient deposition and CO₂ air value).

2.4. Simulations protocol and set-up

Long-term simulations can be affected by drifts in state variables due to the imbalance among boundary conditions, transport processes and internal element cycle formulations of the biogeochemical model. Therefore, a specific simulation protocol, based on the use of a control/scenario ~~pairpairs~~ of simulation, has been implemented in order to disentangle the climate change signal from spurious signals (Solidoro et al., 2024). The protocol consists of a control simulation (CTRL) of 95 years and two 95-year biogeochemical scenario simulations, RCP4.5 and RCP8.5 (Fig.S1 ~~in the supplementary materials~~). All the simulations, which adopt as initial conditions the resulting final fields from ~~thea~~ spin-up simulation (section 2.3). The CTRL ~~is performed by repeatingly reproduces an average condition corresponding to the 2005–2014 physical forcing and river dischargeperiod looped over the remaining 2015-2100 period for both physical forcing and river discharge~~ (Fig. S1). The difference between each biogeochemical scenario and the CTRL provides the future evolution of a biogeochemical variable due to climate forcing.-

Under each specific emission scenario and in the CTRL, our simulation protocol computes the time series of the 3D mean annual dissolved nutrients and oxygen, chlorophyll-a, net primary production, phytoplankton respiration, organic matter, plankton and bacterial biomass, POC, DIC and pH.

First, the annual 3D fields are vertically averaged over two separate key vertical levels: the surface zone and the intermediate zone. The first one spans the upper 100 m of the water column, which represents the location of MAW and the euphotic layer of the basin where most biological activities are concentrated. The second one covers the 200-600 m

level, which includes the location of LIW. Only for the net primary production and phytoplankton respiration, a vertical integral over the 0-200 m layer is considered (Lazzari et al., 2012).

Second, the temporal evolution of the unbiased scenario starting from the present state, $U(k)_{SCEN}$ (with $k = 2005, \dots, 2099$), is defined as:

$$U(k)_{SCEN} = X'_{SCEN} + X(k)_{SCEN} - X(k)_{CTRL} \quad (1)$$

where X'_{SCEN} is the average of $X(k)_{SCEN}$ over the 2005-2020 period (hereafter the PRESENT, Fig.S1), and $X(k)_{SCEN}$ and $X(k)_{CTRL}$ are the yearly average in the scenario and CTRL simulations, respectively. We introduce the concept of "unbiased scenario" because equation (1) removes the effect of potential model drifts due to unbalanced boundary conditions and model errors. The time series of CTRL are filtered with a linear regression to keep the long-term drift and remove spurious variability. The period 2005-2020 has been chosen as reference (also in the forthcoming validation) due to: (i) the availability, after the 2000, of more advanced satellite and assimilated datasets to evaluate the biogeochemistry of the basin, (ii) to avoid the overlapping between historical and scenario part of the simulations (with the latter starting in 2005). It is important to stress here that the choice of the period should not significantly affect the results of the study as the observed differences during this period between the two scenarios for temperature, salinity and current speed fields have been found to be not statistically significant over most of the basin (not shown).

Finally, the temporal evolution of the climate change signal (CCS) with respect to the present is given by:

$$CCS(k)_{SCEN} = U(k)_{SCEN} - U_{SCEN-PRESENT} \quad (2)$$

where $U_{SCEN-PRESENT}$ is the average of $U(k)_{SCEN}$ in the PRESENT. Hereafter, if not differently specified, all the shown time-series will be represented by CCS_{SCEN} .

Horizontal spatial averages are computed considering the sub-basins defined in Fig. 1, the whole Mediterranean basin scale, and two macro-areas: the Western Mediterranean (WMED which includes ALB, SWM, NWM, TYR) and the Eastern Mediterranean (EMED which includes ION and LEV). The Adriatic and Aegean Seas are ~~not~~ usually not considered part of the Eastern Mediterranean due to the importance of local forcing, such as riverine loads, in shaping the variability of the biogeochemical dynamics in those two sub-basins. Because of that, following the approach already adopted in previous works (Lazzari et al., 2012; 2016; Di Biagio et al., 2019; Reale et al., 2020 a,b) they are not considered in the spatial averages related to WMED and EMED.

Temporal averages of the climate change signals are computed over two 20-year periods: 2040-2059, hereafter referred to as "MID-FUTURE" and 2080-2099, hereafter referred to as "FAR-FUTURE" (Fig.S1). The relative climate change signals (in %, except for pH which will be measured in units of pH) in the MID-FUTURE or FAR-FUTURE periods with respect to the PRESENT are computed as:

$$U_{MID-FUTURE} = 100 * (U_{SCEN-MID-FUTURE} - U_{SCEN-PRESENT}) / U_{SCEN-PRESENT} \quad (3)$$

$$U_{FAR-FUTURE} = 100 * (U_{SCEN-FAR-FUTURE} - U_{SCEN-PRESENT}) / U_{SCEN-PRESENT} \quad (4)$$

where $U_{SCEN-MID-FUTURE}$, $U_{SCEN-FAR-FUTURE}$ and $U_{SCEN-PRESENT}$ are the averages of $U(k)_{SCEN}$ for the MID-FUTURE, FAR-FUTURE and PRESENT periods, respectively. Hereafter, if not differently specified, all the percentages shown in the maps are represented by $U_{MID-FUTURE}$ and $U_{FAR-FUTURE}$. The statistical significance of the relative climate change signals in each point of the basin is assessed by means of Mann-Whitney test with $p < 0.05$.

3. Results

3.1 Evaluation of the MFS16-OGSTM-BFM control simulation for the present climate

MFS16 modelling system performances under present climate conditions were previously analyzed (Lovato et al., 2013; Galli et al., 2017), showing that the main spatial-temporal characteristics of the Mediterranean Sea physical properties reliably compared against ocean reanalysis datasets. circulation and spatial patterns, mean values and standard deviations of temperature and salinity at different depths in the basin were reliably reproduced (Lovato et al., 2013; Galli et al., 2017). Moreover, the physical reanalysis dataset produced by MFS16 within the Copernicus Marine Environmental Marine Service (CMEMS) (Simoncelli et al., 2019) has already been coupled to the transport-reaction model OGSTM-BFM to carry out a reanalysis for the Mediterranean Sea biogeochemistry (Teruzzi et al., 2019). The latter is a biogeochemical dataset covering the 1999-2015 period at 1/16° resolution, which was already used for validating different biogeochemical simulations in the Mediterranean Sea, such as those based on MEDMIT12-BFM (Mediterranean MIT General circulation Model-BFM at 1/12°; Di Biagio et al., 2019) and RegCM-ES (Regional Climate Model-Earth System; Reale et al., 2020a) modelling systems. This dataset has been recently upgraded, refining the resolution to 1/24 degree and extending the period to 2019 (Teruzzi et al., 2021; Cossarini et al., 2021).

To date, no future climate biogeochemical projection of the Mediterranean Sea has been performed through this offline coupling.

Figure 2 a,b shows the surface average chlorophyll-*a* (Chl-*a*) concentrations (upper 10 m) from the CTRL run compared with a climatology based on satellite data available from CMEMS which covers the period 1999-2015 (Colella et al., 2016). The model correctly reproduces the areas in the Mediterranean region characterized by relatively high values of Chl-*a*: the Alboran Sea, the Gulf of Lion, the coastal areas of the Adriatic Sea, and the Strait of Sicily. Moreover, the CTRL simulation captures the west-east trophic gradient of Chl-*a*, whose existence has been pointed out in previous works (D'Ortenzio and Ribera d'Alcala, 2003; Lazzari et al., 2012; Colella et al., 2016; Richon et al., 2019; Di Biagio et al., 2019; Reale et al., 2020a). On the other hand, we observe a general underestimation of approximately 50% of the Chl-*a* signal throughout the basin and in the coastal areas is observed, probably associated with insufficient river load (Richon et al., 2019; Reale et al., 2020a) and with the tendency of satellite Chl-*a* measures to be systematically overestimated in the coastal areas with respect to “in situ” observations due to the presence of particulate suspended matter in the water column (Claustre et al., 2002; Morel et Gentili, 2009).

Figure 2 also shows the average vertical profiles, computed for the entire, Western and Eastern Mediterranean basins, of Chl-*a* (c), PO₄ (d), NO₃ (e), dissolved oxygen (f), DIC (g), pH (h) and Total Alkalinity (i) in the CTRL compared with the recent CMEMS reanalysis (only for Chl-*a* and pH, Cossarini et al., 2021) and EMODnet datasets (European Marine

379 Observation and Data Network; Buga et al., 2018). In spite of the tendency to overestimate the Chl-a values, ~~t~~The model
380 captures the DCM location, the west-east trophic gradient in the basin, and also the nutricline depths deepening between
381 Western and Eastern basin and the low nutrient surface concentrations. Mean simulated values in the first 0-200 m are
382 quite realistic for almost all the biogeochemical tracers and properties, with correlation ~~values~~coefficient between
383 observations and modelled data greater than 0.93. At the same time, the CTRL overestimates the PO₄ concentration
384 between 100 and 300m of about 50%, and the dissolved oxygen concentration of about 15% below 200 m and
385 underestimates, below 200 m, the NO₃ concentration of about 20% and the pH of about 1 % between 100 and 300m. It is
386 worthwhile to point out the limited spatial ~~low~~ resolution of the observations below 200 m ~~that~~ could impact ~~make the~~
387 robustness of our comparison ~~less robust~~. In general, ~~these~~ biases in the initial conditions are originated by ~~come from~~
388 the spin-up simulation that allows to remove the largest part of ~~the~~ model drifts ~~to be removed~~. As explained in section
389 2.4, these biases, Biases which are still present in both the CTRL and scenario simulations, do not affect the calculation
390 of the climate change signals, and are generally ~~while the eventually still present drifts in the CTRL are by far~~ lower than
391 the changes observed in the scenarios at the end of the century climate signal.

392 To summarize, although the model shows some deficiencies in simulating the vertical distribution of some
393 biogeochemical tracers and properties, the main ~~biogeochemical~~ features of the ~~system~~basin are reliably ~~very well~~
394 simulated and thus, MFS16-OGSTM-BFM is robust enough ~~to can~~ be used to investigate the evolution of the
395 Mediterranean biogeochemistry under different emission scenarios.

396

397

398

399

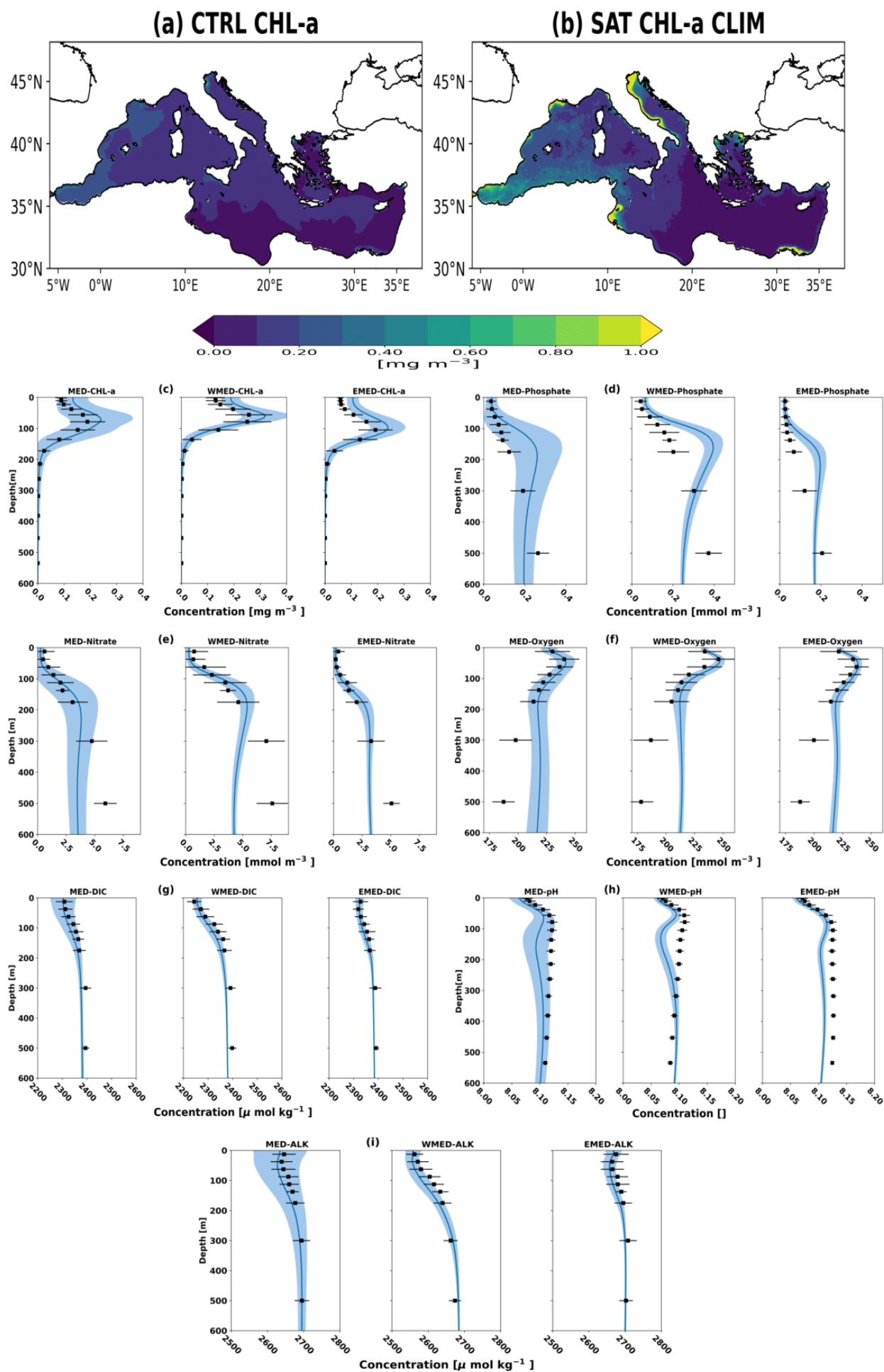


Fig.2 Average Chl-a in the first 10m in CTRL (a) for the period 2005-2020 and CMEMS-SAT (b) together with CTRL average vertical profiles (blue lines) for the period 2005-2020 of Chl-a (c, mg m^{-3}), PO_4 (d, mmol m^{-3}), NO_3 (e, mmol m^{-3}), Dissolved oxygen (f, mmol m^{-3}), DIC (g, $\mu\text{mol kg}^{-1}$), pH(h) and total alkalinity (i, $\mu\text{mol kg}^{-1}$). The averaged profiles are computed for the entire (MED), Western (WMED) and Eastern (EMED) Mediterranean Sea. The light blue areas represent the spatial standard deviation of the monthly model data. The model data are compared with CMEMS reanalysis (Chl-a and pH; Colella et al., 2016; Teruzzi et al., 2021) and observations provided by EMODnet (PO_4 , NO_3 , Dissolved oxygen, DIC, total alkalinity; Buga et al., 2018): annual mean (black squares) and related standard deviations (black bars). Depth is measured in meters.

3.2 Evolution of the thermohaline properties and circulation of the Mediterranean Sea in the 21st century

Mean temperature and salinity evolution between 0-100 m and 200-600 m in the 2005-2099 period under the RCP4.5 and RCP8.5 scenarios in the whole Mediterranean Sea and in the Western and Eastern basins are shown in Fig. 3. As for the biogeochemical variables, these depths have been chosen as they are representative of the location of MAW and LIW, respectively.

A warming of the surface and intermediate layers is observed at the basin scale and in both the ~~western~~Western and ~~eastern~~Eastern basins, whose magnitude (approximately 1.5o C in the RCP4.5 and 3°C in the RCP8.5 scenario), agrees with what has already been observed in recent modelling studies based on single/multimodel ensembles (e.g., Adloff et al., 2015; Soto-Navarro et al., 2020).

Similar to the seawater temperature, the variation in salinity is strongly dependent on the emission scenario with more intense anomalies, both negative and positive, under RCP8.5 conditions (as observed in previous modelling studies such as Adloff et al., 2015 and Soto-Navarro et al., 2020). For example On the other hand, the salinity in the surface layer at basin scale and in the ~~eastern~~Eastern basin is characterized by a decrease between 2020 and 2050 followed by a constant increase (stronger under in the RCP8.5 scenario) until the end of the 21st century. Conversely, after 2050, the Western basin shows a freshening of the surface layer with respect to the beginning of the century, in agreement with what was already observed by Soto-Navarro et al. (2020). An increase in salinity also occurs in both scenarios in the intermediate layer both at the basin scale and in the two main sub-basins. Conversely, after 2050, the westernWestern basin shows a freshening of the surface layer with respect to the beginning of the century, in agreement with what was already observed by Soto-Navarro et al. (2020). Similar to the seawater temperature, the variation in salinity is strongly dependent on the emission scenario with more intense anomalies, both negative and positive, under RCP8.5 conditions (as observed in previous modelling studies such as Adloff et al., 2015 and Soto-Navarro et al., 2020).

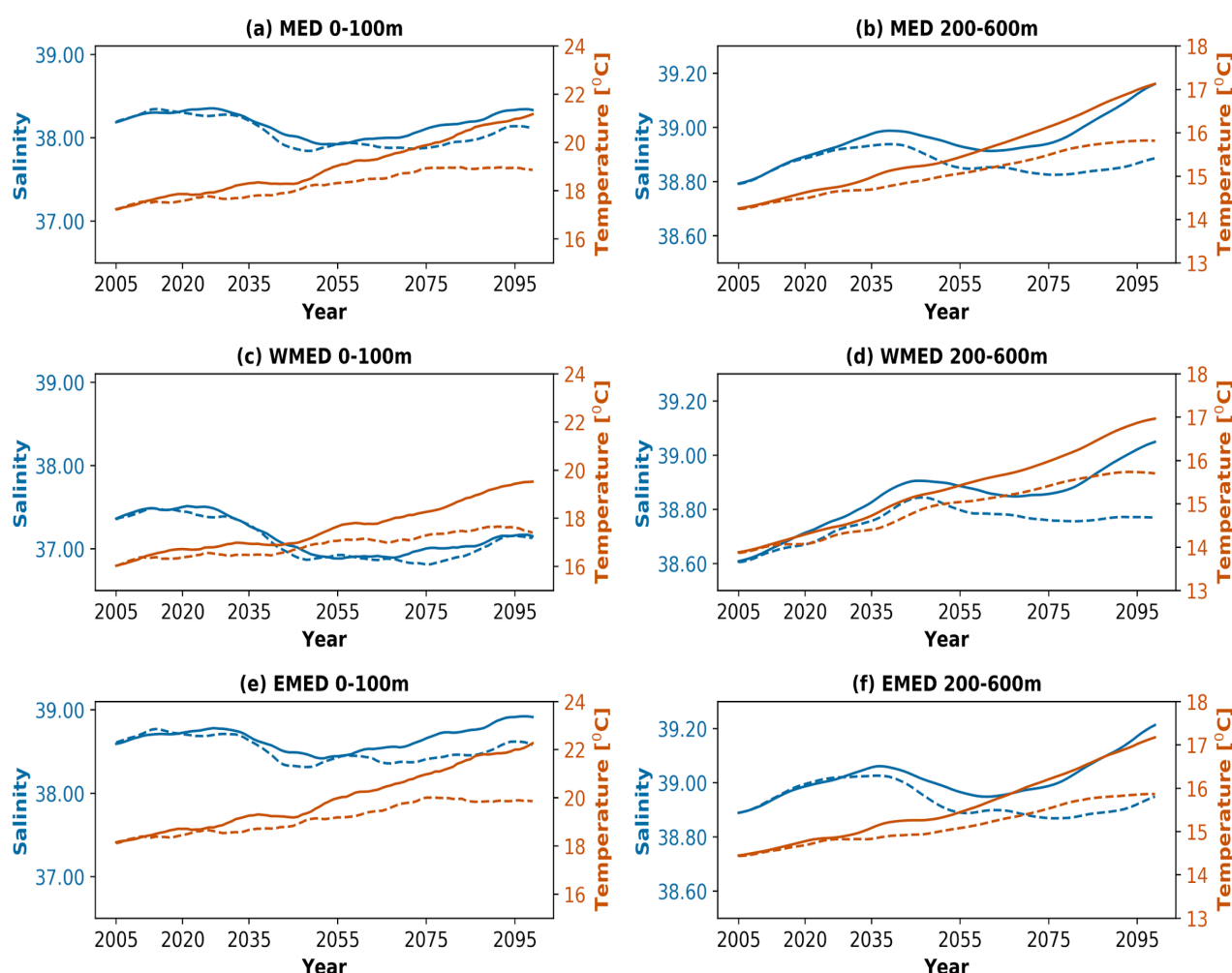


Fig.3 - Yearly ~~timeseries~~time-series for the period 2005-2099 of Salinity (blue) and Temperature (dark orange, in °C) under the emission scenarios RCP8.5 (solid line) and RCP4.5 (dashed line) in the Mediterranean Sea (MED, a-b), ~~Western~~Western Mediterranean (WMED, c-d) and ~~Eastern~~Eastern Mediterranean (EMED, e-f) for the layers 0-100 m (left column) and 200-600 m (right column). The yearly ~~timeseries~~time-series have been smoothed using 10-years running mean.

The spatial distribution of temperature variations in the surface layer (Fig. S2) shows a comparable and mostly statistically significant on basin-scale warming in RCP4.5 and RCP8.5 in the MID-FUTURE (the differences between the projected changes are lower than 2%), while, in the FAR-FUTURE, the projected changes in the RCP4.5 are approximately the 50% lower with respect those observed observed in RCP8.5 (8-12% and 17-20% respectively), with the North Western Mediterranean, Tyrrhenian, Adriatic, Ionian, Aegean Sea and Levantine being the most affected sub-basins. Local relative maxima are observed in both scenarios, in the Gulf of Lion, in the relatively shallow and coastal areas of the Adriatic Sea and in the area of the Rhodes Gyre (Fig.S2 i,j).

The spatial distribution of temperature and salinity variations in the surface layer (Fig. S2 and Fig. S3 in the supplementary materials) shows a comparable and mostly statistically significant on basin-scale warming in RCP4.5 and RCP8.5 in the MID-FUTURE (the differences between the projected changes are loweress than 2%) and a half a doubled FAR-FUTURE variation in RCP4.5 (8-12%)RCP8.5 (17-20%) with respect to RCP4.5 (8-12%)RCP8.5 (17-

20%), with the north western Western Mediterranean, Tyrrhenian, Adriatic, Ionian, Aegean Sea and Levantine being the most affected sub-basins. Local relative maxima are observed in both scenarios, in the Gulf of Lion, in the relatively shallow and coastal areas of the Adriatic Sea and in the area of the Rhodes Gyre (Fig. S2 i,j). Similar relative variations are observed in the intermediate layer (Fig. S2).

A general freshening of the upper layers and saltening of the intermediate layers are observed over most of the entire Mediterranean basin is observed during the MID-FUTURE period (Fig. S3). The projected changes are statistically significant over most of the basin with the only exception, in both scenarios, in both scenarios of the upper layer surface of the Adriatic Sea and Northern Ionian Sea and the intermediate layers of the Southern Ionian and Levantine Basin/Southern Adriatic and Northern Ionian Sea in the RCP4.5/RCP8.5 scenario as consequence, probably, of the river input in the Adriatic Sea and mid-Ionian Jet dynamics. The latter has been recognized, in fact, as an important driver for the salinity for the upper and intermediate layers of the Adriatic and Ionian Sea (e.g. Gacic et al., 2010). General freshening/saltening of the upper/intermediate layers is observed over the entire basin during the MID-FUTURE period (Fig. S3 in the supplementary materials). In the FAR-FUTURE, the freshening of the surface is still present at the basin scale in the RCP4.5 scenario (although it is reduced with respect to the MID-FUTURE) and in the western Western basin in the RCP8.5 scenario. Moreover, an increase in salinity is observed in the Adriatic Sea (in both scenarios) and in the eastern Eastern basin under RCP8.5. T On the other hand, the projected changes in the surface salinity in the Adriatic Sea and Northern Ionian Sea under RCP4.5 at the surface are also still not significant.

The decrease in salinity in the 21st century in the western Western basin is driven by the salinity values imposed in the Atlantic buffer zone (Lovato et al., 2013), while the saltening of the eastern Eastern basin, under RCP8.5 scenario, is linked to the increased freshwater deficit decreasing freshwater discharge in the area (e.g., Gualdi et al., 2013; Soto-Navarro et al., 2020). In the intermediate layer, the situation is reversed: while in RCP8.5, the entire basin experiences an increase in the salinity associated with the increase in salinity in the surface water of the eastern Eastern basin, in RCP4.5, the eastern Eastern basin experiences a slight decrease in salinity associated again with the freshening of surface water. In fact, at the surface, both signals are transported by vertical mixing to the intermediate layers of the eastern Eastern basin influencing the salinity of the newly formed LIW.

Figure 4 shows the temporal evolution of the Mediterranean thermohaline circulation during the 21st century using the zonal overturning stream function (or ZOF; Myers and Haines, 2002; Somot et al., 2006). The ZOF has been computed by the meridional integration from south to north and from the bottom to the top of the water column of the zonal velocity (see Adloff et al., 2015). The domain of the integration is the same as shown in Figure 1 with the exclusion of the Atlantic area outside the Strait of Gibraltar strait. The thermohaline circulation of the basin in the PRESENT is composed of two cells, similar to the outcomes of the historical reference experiments described in Adloff et al. (2015) and Waldman et al. (2018). The first cell extends from the surface to 800 m, with a clockwise circulation associated with MAW moving eastwards and LIW moving westwards. The second cell is located between 500 and 2500 m in the eastern Eastern Mediterranean with a counterclockwise circulation associated with the Eastern Eastern Mediterranean Deep Water (EMDW) moving eastwards and LIW moving westwards.

495 Under the two scenarios, during the MID-~~FUTURE~~FUTURE period, there is an evident weakening of both cells and a
496 reduction of the thickness of the upper layer cell and the ~~eastern~~Eastern basin cell (less than -0.1 Sv), which splits into
497 two sub-cells. By the end of the century both cells show a similar ~~behavior~~behaviour, whereas in the RCP4.5 scenario,
498 the ~~eastern~~Eastern cell is slightly more intense. The weakening of the zonal overturning stream function is similar to
499 previous findings of Somot et al. (2006) and Adloff et al. (2015). As the Mediterranean thermohaline circulation is driven
500 by both deep and intermediate water formation processes, the overall weakening of both cells is a direct consequence of
501 the increase in the vertical stratification of the water column. In fact, the evolution of the winter maximum mixed layer
502 depth in key convective areas of the Mediterranean Sea, such as the Gulf of Lions, Southern Adriatic, Aegean Sea and
503 Levantine basin (Fig. S4 ~~in the supplementary materials~~), shows a progressive decrease in the intensity of the open ocean
504 convection after 2030. Only for the Aegean Sea, ~~are~~ the changes in the winter mixed layer maximum depth are less
505 marked, with the occurrence of some maxima around 2080 (in RCP8.5) or after 2090 (in RCP4.5), which could correspond
506 to a future tendency of the thermohaline circulation of the ~~Eastern~~Eastern basin to produce EMT (Eastern Mediterranean
507 Transient)-like events (Adloff et al., 2015).

508
509 The projected overall weakening of the Mediterranean thermohaline circulation leads to a reduction in the exchanges of
510 biogeochemical properties between the ~~western~~Western and ~~eastern~~Eastern basins through the Strait of Sicily ~~strait~~ at
511 both the surface and intermediate levels (Fig.S5 ~~in the supplementary materials~~) and to a reduced ventilation of
512 intermediate/deep waters (Adloff et al., 2015).

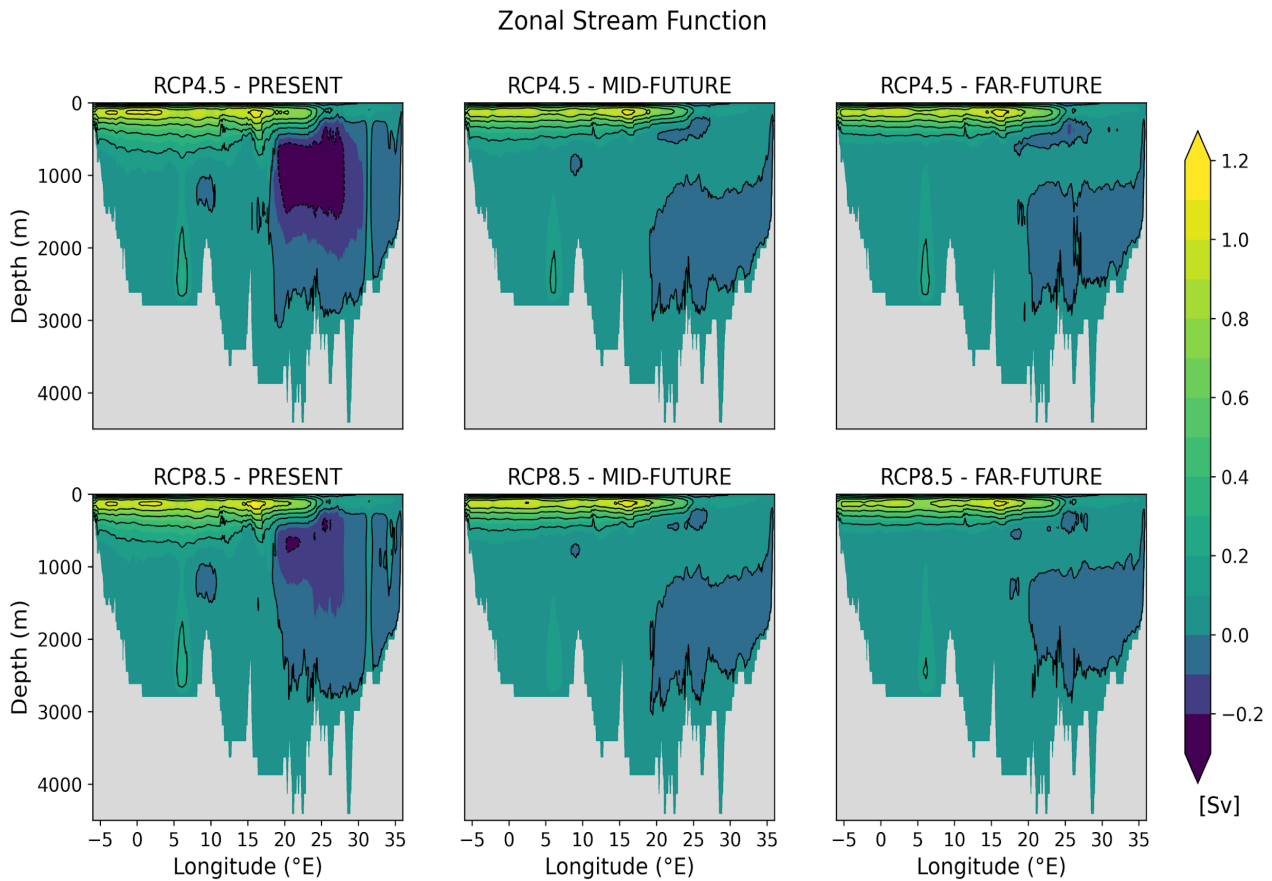


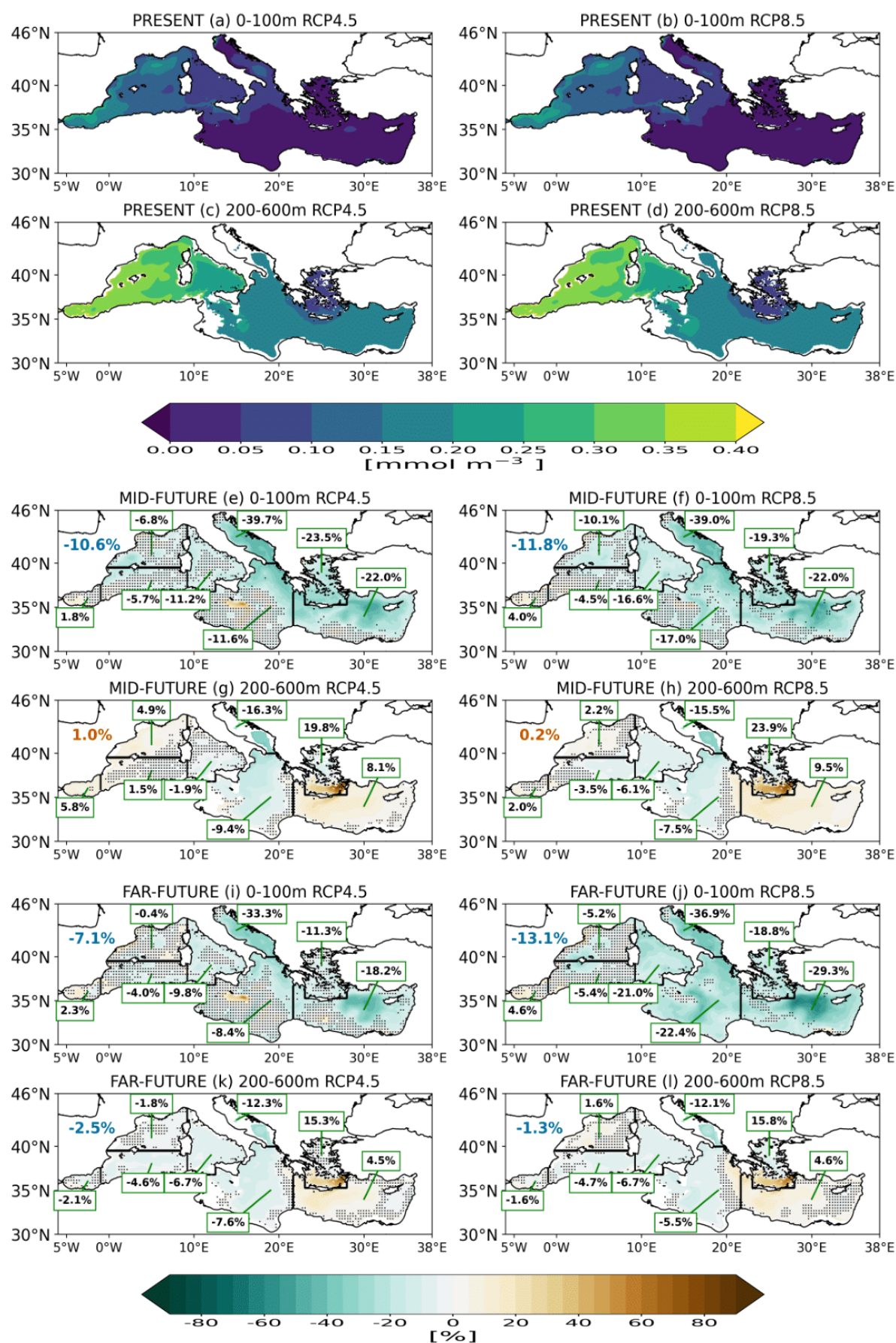
Fig. 4 - Mediterranean Sea zonal stream function annual mean (in Sv) averaged over the PRESENT (2005-2020), MID-FUTURE (2040-2059) and FAR-FUTURE (2080-2099) periods under RCP4.5 and RCP8.5 scenarios.

3.3 Spatial and temporal evolution of nutrients, dissolved oxygen and chl-*a* concentrations

Figures 5 and 6 show the spatial distribution of the magnitude and signs of the changes that will affect the dissolved nutrient concentrations during the 21st century. In the FAR-FUTURE, the decreases in PO_4 and NO_3 concentrations in the 0-100 m layer under the RCP8.5 scenario are almost half in double RCP4.5 (approximately 7% and 13% for PO_4 and NO_3 , respectively) (approximately 13% and 20% for PO_4 and NO_3 , respectively) with respect to those observed in the RCP4.5 (approximately 7% and 13%) RCP8.5 (approximately 13% and 20% for PO_4 and NO_3 , respectively) and are particularly marked and statistically significant in the Levantine basin, in the Aegean Sea, and in the Central/Southern Adriatic Sea and Tyrrhenian Northern Ionian Sea. Again, statistically significant relative local maxima (in absolute value) maxima are observed in both scenarios in the area of the Gulf of Lion, Southern Adriatic, Northern Ionian and Rhodes Gyre. Moreover, there are clear spatial gradients affecting the existence of spatial gradients in the statistical significance of the projected changes within the same sub-basin of the Mediterranean Sea. For example, the projected changes in nutrient concentration an overall increase (stronger in of NO_3 concentration is than PO_4) is projected observed in the Northern Adriatic Sea and in many other coastal areas influenced by river dynamics are not significant, contrary to what is observed in the open ocean areas of the same sub-basin. Here This signal can be explained by the increase in vertical stratification and the decrease in river discharges (Gualdi et al., 2013) which results in a higher

concentration of the nutrients at the river mouths. The increase in the Northern Adriatic is counterbalanced by a ~~the~~ projected decrease ~~in the Southern Adriatic~~ associated with the reduced vertical mixing in the water column and reduced inflow of nutrients through the Otranto Strait (Fig. S6 ~~in the supplementary materials~~). ~~Finally~~ Moreover, the two scenarios show some significant changes in the dissolved nutrient concentrations at local scale (~~brown patches~~) in the Alboran Sea and in the ~~S~~southern Ionian associated with changes in the intensity of mesoscale circulation (eddies) of both areas and in the intensity and spatial structure of the mid-Ionian jet (not shown).-

In contrast to the general decreasing nutrient content of the upper layer, the intermediate layer in both scenarios shows a strong (milder) increase in nutrient concentration in the ~~S~~southern Aegean Sea (Levantine basin, ~~N~~orth~~western~~ Western Mediterranean and Alboran Sea) in the 21st century driven by the reduced vertical mixing, which tends to increase the nutrient content of the intermediate layers. The Tyrrhenian, Ionian and Southern Adriatic Seas are, in turn, characterized by a permanent negative anomaly. In the first two areas, the anomaly can be associated with the decrease in the westward transport of nutrients in the intermediate layers through the Sicily Strait (consequences of the weakening of the zonal stream function discussed in Section 3.2, Fig. S5), while in the Adriatic Sea, the ~~projected~~observed changes are driven by the increase in the nutrient export in the intermediate layer through the Otranto Strait (Fig. S6). In the ~~N~~orth~~western~~ Western Mediterranean, the observed positive anomalies become weaker and even negative in the FAR-~~FUTURE~~FUTURE under the RCP4.5 emission scenario, likely due to some convective events that take place between 2080 and 2100, as shown in Fig. S4. Comparing the projected changes at the surface in the FAR-FUTURE at the surface in both scenarios is clearly a strong difference among the two: while it is observed that while under RCP4.5 in most of the Western Mediterranean and the Ionian Sea the projected changes are keep to be not statistically significant significant with respect to the PRESENT, under RCP8.5 emission scenario the statistical significance projected changes that which that were initially limited to Adriatic, Aegean Sea and Levantine basin, now it also will involves also the Ionian and Tyrrhenian Sea.



560
561
562
563
564
565
566
567

Fig. 5 - Phosphate concentration (in mmol m⁻³) in the layers 0-100 m and 200-600 m in the PRESENT (2005-2020, a,b,c and d), and relative climate change signal (with respect to the PRESENT) in the MID-FUTURE (2040-2059, e,f,g and h) and FAR-FUTURE (2080-2099, i,j,k and l) in the RCP4.5 (left column) and RCP8.5 (right column) emission scenario. The Mediterranean average relative climate change signal in each period (with respect to the PRESENT) is displayed by the top-left colored value (blue or dark orange when negative or positive). Values in the green boxes are the average relative climate change in each period and in each sub-basin shown in Figure 1. Domain grid points where the relative climate change signals are not statistically significant according to a Mann-Whitney test with $p < 0.05$ are marked by a dot.

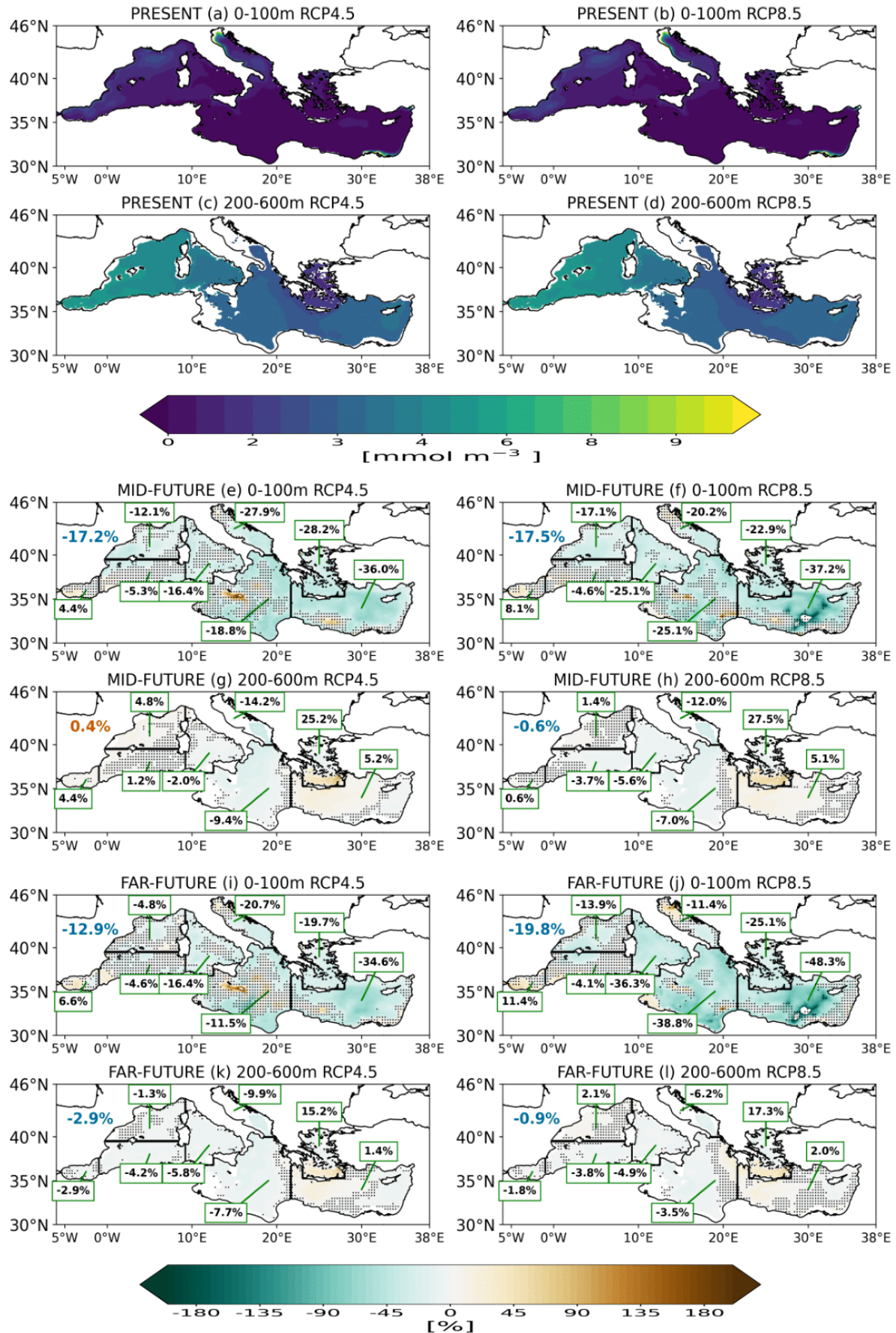


Fig.6 - as Fig.5 but for Nitrate (in mmol m⁻³)

The temporal evolution of the mean concentrations of PO₄ and NO₃ in the RCP4.5 and RCP8.5 simulations between 0-100 m and 200-600 m in the Mediterranean Sea and its ~~western~~Western and ~~eastern~~Eastern basins for the 2005-2099 period is shown in Fig. 7. In the RCP8.5 scenario, PO₄ and NO₃ concentrations within the euphotic layer of both sub-basins are substantially stable for the first 30 simulated years, while a marked decline occurs after 2030-2035, with values of 0.01 and 0.1 mmol m⁻³ (compared to the beginning of the century) respectively, which is followed by a steady evolution of the concentration values until the end of the century. The same behaviour is observed in RCP4.5, except for a recovery that takes place at the end of the century in correspondence to an increase in the nutrient inflow ~~into the Alboran Sea at the Strait of Gibraltar~~Gibraltar strait (Fig. S7 ~~in the supplementary materials~~). The observed decline is timely in phase with the weakening of the zonal stream function discussed in Fig. 4, further pointing out the importance of ~~the~~ vertical mixing in driving the temporal variability of nutrients in the euphotic layer. From this point of view, some relative maxima of both nutrient concentrations in the ~~western~~Western and ~~eastern~~Eastern basins are observed for RCP4.5 in the 2015-2040 period (Fig. 5 c,d), associated with strong ocean convective events taking place in the Gulf of Lions and Levantine basin (Fig. S4). ~~Between 2055 and 2075, the peak in both nutrients' concentration, for RCP4.5, timely corresponds to a peak in the inflow of nutrients into the Alboran Sea (Fig. S7). Additionally, in both the scenarios, the intermediate layer of the Western basin, after 2035, experiences a negative tendency in the nutrient concentration (greater than 0.01 mmol m⁻³ for PO₄ and 0.1 mmol m⁻³ NO₃) related to a reduced westward transport of nutrients associated with LIW (Fig.S5). The peak in both the nutrients concentration, between 2055 and 2075, in RCP4.5 timely corresponds to a peak in the inflow of nutrients at the Strait of Gibraltar~~Gibraltar strait (Fig. S7). Additionally, ~~the intermediate layer of the western basin, in both scenarios, after 2035 experiences by a negative tendency in the nutrient concentration which is greater than 0.01 mmol m⁻³ for PO₄ and 0.1 mmol m⁻³ NO₃, related to a reduced westward transport of nutrients associated with LIW (Fig.S5).~~

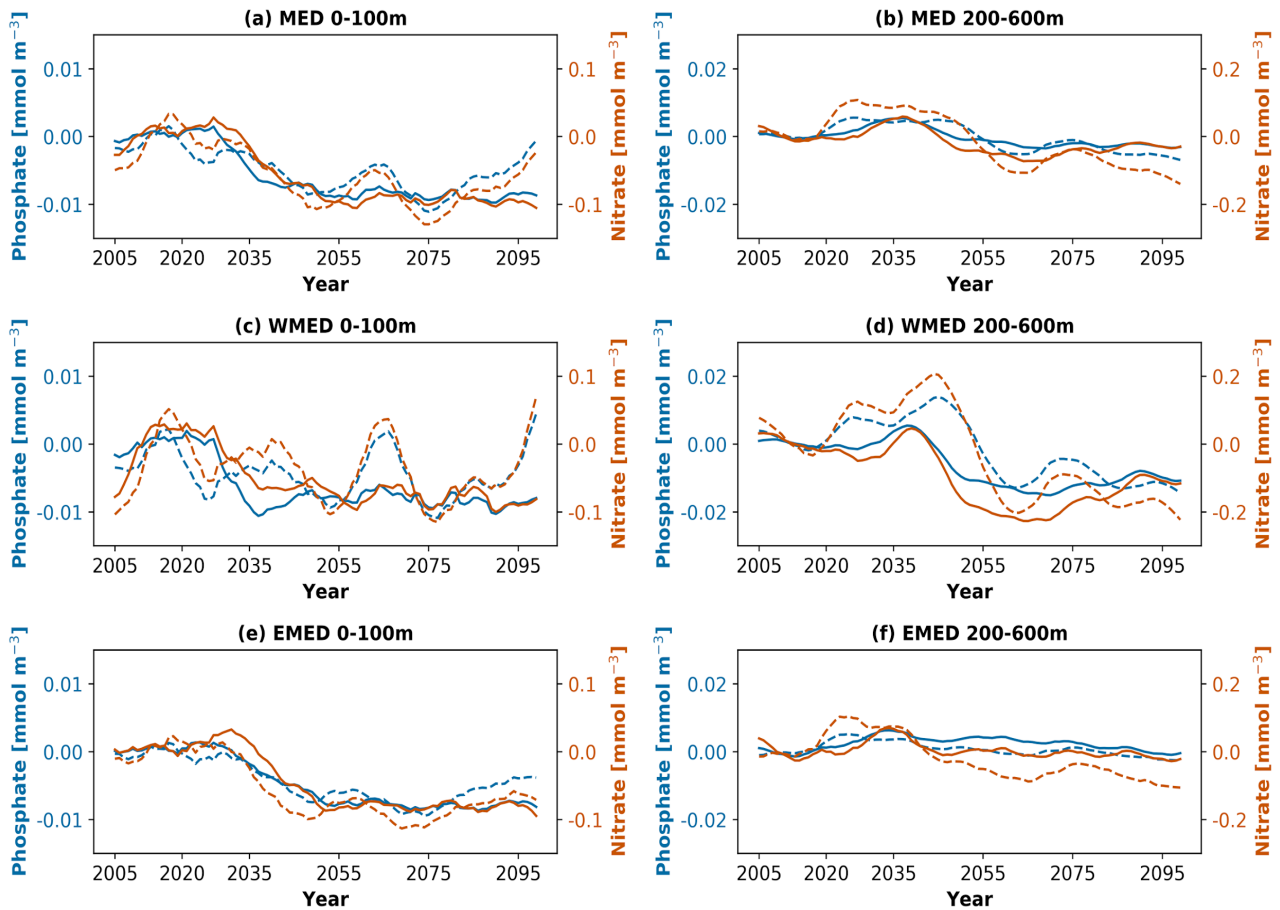


Fig.7 - Yearly time-series for the period 2005-2099 of Phosphate (blue, in mmol m⁻³) and Nitrate (dark orange, in mmol m⁻³) anomalies for the emission scenario RCP8.5 (solid line) and RCP4.5 (dashed line) in the Mediterranean Sea (MED, a-b), WesternWestern Mediterranean (WMED, c-d) and EasternEastern Mediterranean (EMED, e-f) for the layer 0-100_m (left column) and 200-600_m (right column). The yearly time-series have been smoothed using 10-years running mean.

The temporal evolution of chlorophyll-*a* in the two scenarios is similar to what was observed in the case of dissolved nutrients, with a high interannual variability, a decrease after 2030-2035 of approximately 0.03 mg m⁻³ and a stable signal until the end of the century in the RCP8.5 scenario while, in the case of the with RCP4.5 as the only exception, where a recovery towards the observed PRESENT values is again simulated at the end of 21st centuryobserved (Fig.8). In the easternEastern Mediterranean the decrease is of the same magnitude as that observed at the basin scale, while in the westernWestern basin the chl-*a* signal appears substantially stable with respect to the present.

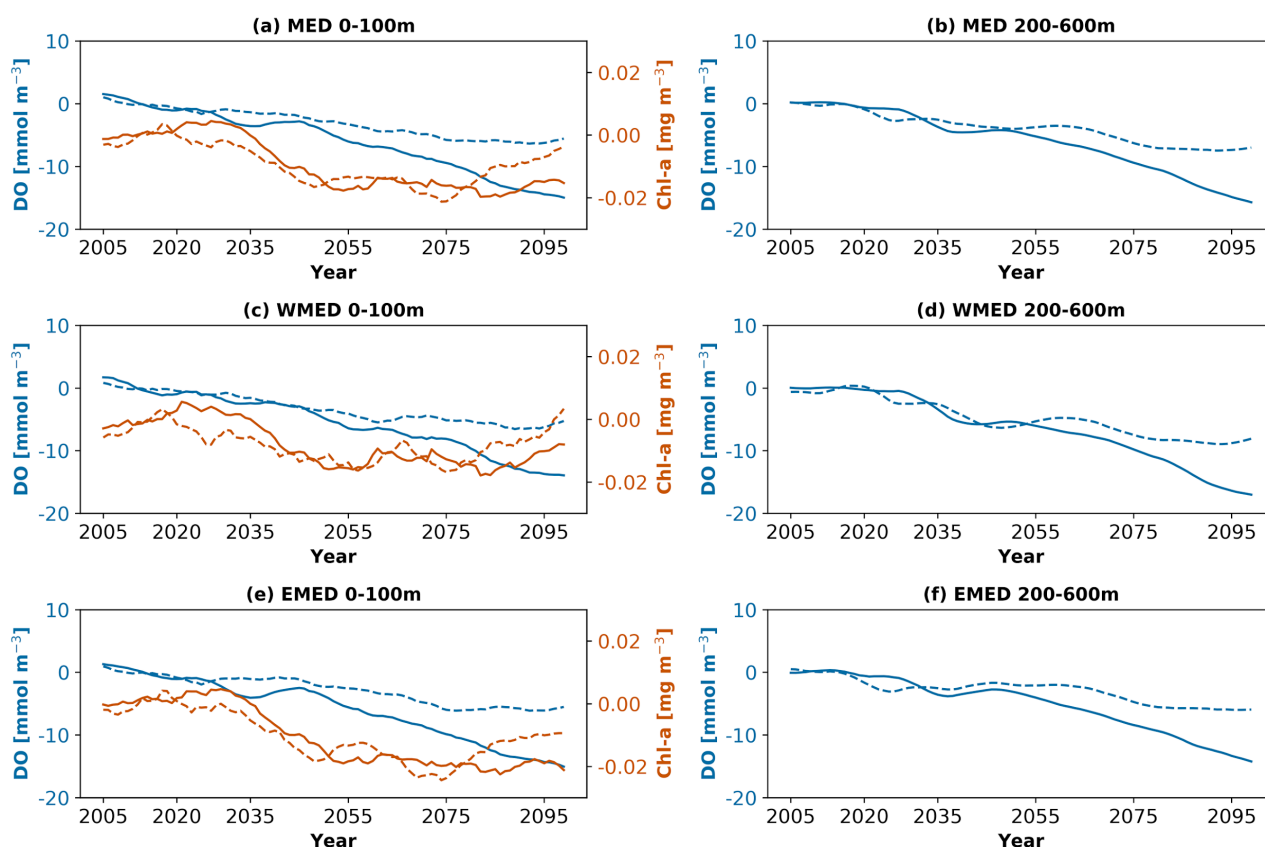


Fig. 8 as Fig.5 but for Dissolved Oxygen (blue, in mmol m^{-3}) and Chlorophyll-*a* (dark orange, in mg m^{-3})

During the 21st century, a continuous decrease in the oxygen concentration is projected in both scenarios in the Mediterranean Sea (Fig. 8). The simulated observed reduction of in the oxygen values solubility is slower in the RCP4.5 with respect to RCP8.5. For example, under the RCP8.5 emission scenario, the concentration of the dissolved oxygen in the upper layer decreases by approximately 15 mmol m^{-3} , which is three times the value observed in the RCP4.5 scenario (Fig. 8). The decrease in dissolved oxygen is rather uniform and almost statistically significant everywhere in both the horizontal and vertical directions in all the sub-basins, with values that are half double in RCP4.5 (in percentages) with respect to those observed under RCP8.5 (Fig. S8, see the supplementary material). For example, the decrease in the oxygen concentration solubility in the Levantine basin, in the FAR-FUTURE FUTURE, is approximately equal to 36% under the RCP4.5 emission scenario and 63% under the RCP8.5 emission scenario. In the North western Western Mediterranean, these values are approximately 37% and 73% respectively. The projected decreases in both scenarios are usually lower in the Alboran Sea and South Western Mediterranean with respect to the rest of the basin, as a consequence of the damping effect driven by the oxygen values imposed at the Atlantic boundary. In fact, the advection of dissolved oxygen associated with Atlantic Water partially limits the reduction in the oxygen solubility at the surface as a consequence of the warming of the water column in the sub-basins near the Strait of Gibraltar, such as the Alboran Sea.

The uniform decrease in the oxygen surface concentration observed in Fig. S8 is spatially coherent (also from the statistical point of view) with the increase in the temperature shown in Fig. S4, confirming the importance of temperature in driving the solubility of the oxygen in the marine environment (Keeling et al., 2010; Shepherd et al., 2017). Moreover,

we also found a decrease in the oxygen inflow (not shown) into the Alboran Sea through the Strait of Gibraltar and an overall increase in community respiration (see the analysis related to the phytoplankton respiration in section 3.4) are found, which represent additional factors explaining the projected changes. Western sub-basins, and deep convection areas and shallow coastal zones of the Adriatic Sea are the regions that show the highest decrease of oxygen in both surface and the intermediate layer, with again the magnitude of the observed signal depending on the scenario that is considered (Fig. S8) and related to the reduction in vertical processes' intensity. The effect of the increased stratification on the oxygen vertical distribution is clearly shown in Figure 9. Under RCP8.5 (Fig. 9 a,b), the progressive decline of oxygen concentration is timely corresponding to the progressive decrease in the maximum mixed layer depth (Fig. S4) and the weakening of the zonal stream function (Fig. 4) discussed in Section 3.2. For example, in the North-Western Mediterranean the correlation coefficient between the average dissolved oxygen concentration in the first 100m and the maximum mixed layer depth has been found equal to 0.64 (statistically significant with $p < 0.05$). On the other hand, under the RCP4.5 emission scenario, some events of deep transport of oxygen, that dumped the decline in the oxygen concentration, can be recognized towards the end of the 21st century in both Western and Eastern Mediterranean sub-basins (for example towards the end of the 21st century).

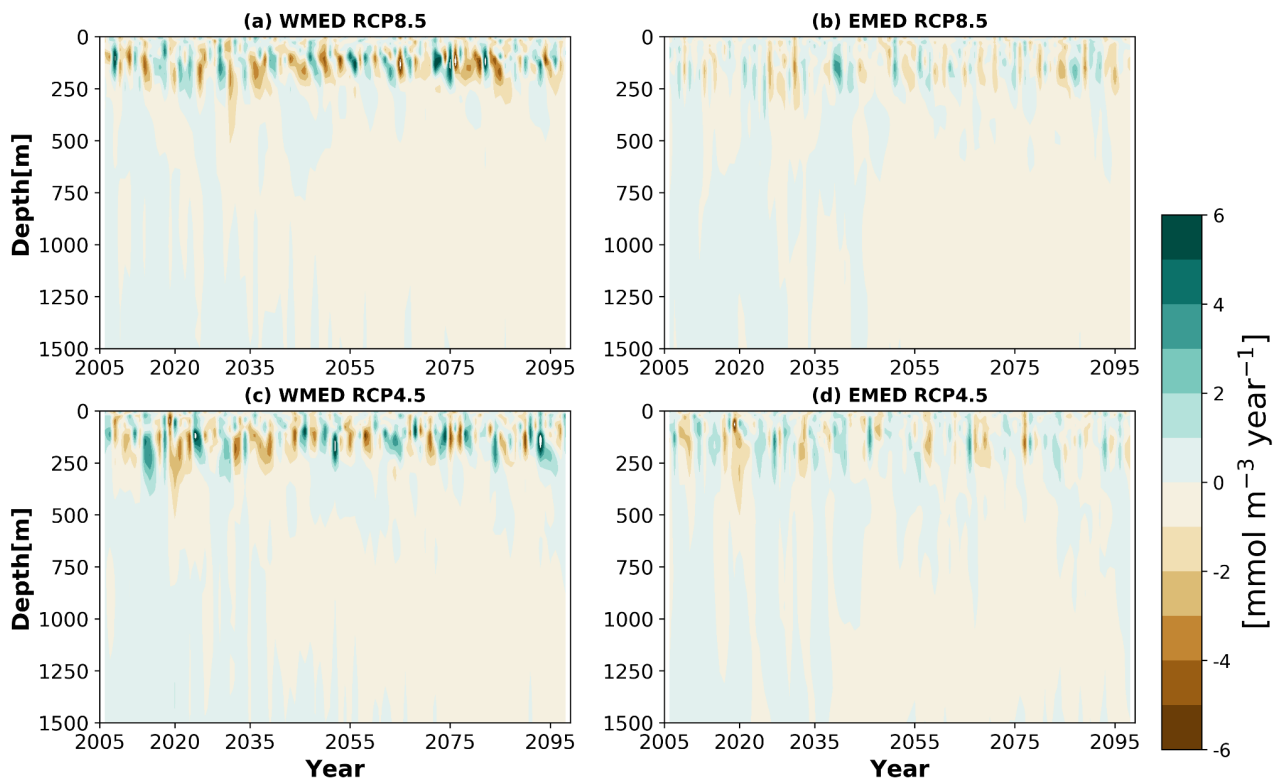


Fig.9 Annual rate of change of Dissolved Oxygen (mmol m⁻³ year⁻¹) in the western (a,c) and eastern (b,d) Mediterranean Sea in RCP8.5 (a,b) and RCP4.5 (c,d).

3.4 Spatial and temporal evolution of net primary production and living/non-living organic matter

The warming of the water column and the increase in vertical stratification affect the metabolic rate of ecosystem processes including CO₂ fixation and community respiration. In fact, a basin-wide increase in net primary production

(NPP) starting after 2035 and proceeding until the end of the simulations, is projected in both the scenarios (Fig. 10). In the RCP4.5 scenario the NPP increase is greater than $120 \text{ gC m}^{-2} \text{ year}^{-1}$, which is a value that is more than half double with respect to the values observed in the RCP8.5 simulation.

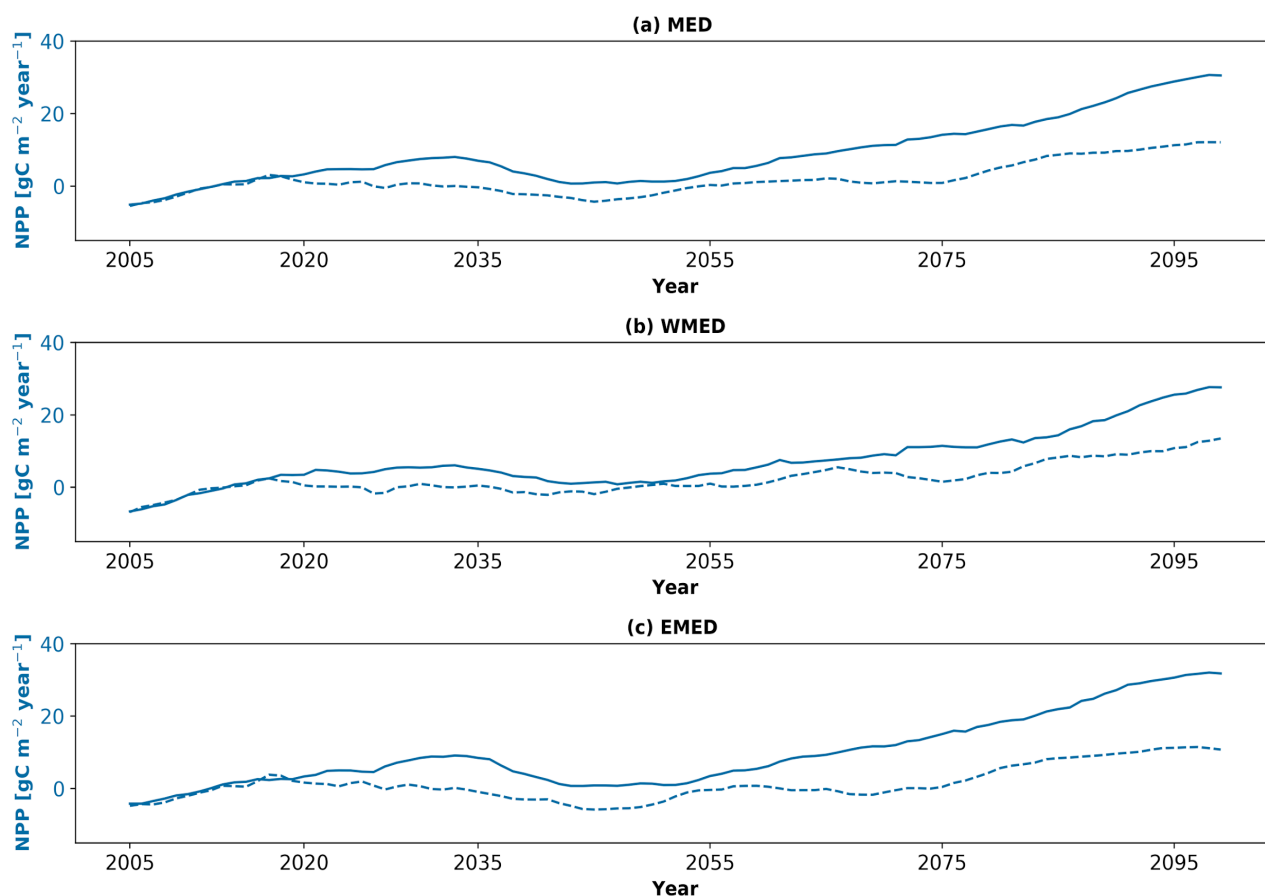


Fig.10 - Yearly time-series for the period 2005-2099 of Integrated net primary production (blue, in $\text{gC m}^{-2} \text{ year}^{-1}$) anomalies for the emission scenario RCP8.5 (solid line) and RCP4.5 (dashed line) in the Mediterranean Sea (MED, a), Western Mediterranean (WMED, b) and Eastern Mediterranean (c) for the first 200 m. The yearly timeseries have been smoothed using 10-years running mean.

The distribution of the sign of the NPP changes is not uniform across the basin and between the simulations (Fig. 11). In the MID-FUTURE, in both scenarios, the only areas that experience an increase (not statistically significant in all the cases) in the NPP with respect to the beginning of the century are the Northwestern Western Mediterranean, the Tyrrhenian Sea, the Northern Adriatic Sea, part of the Ionian Sea and of the Levantine basin. Conversely, the only statistically significant projected changes are negative and are observed in the Central and Southern the rest of the Adriatic Sea, part of the Northern Ionian Sea and the Rhodes Gyre areas show negative anomalies. The Aegean Sea shows a rather opposite behavior with a negative/positive anomaly in RCP4.5/RCP8.5. In the FAR-FUTURE, corresponding to a more pronounced warming of the basin, the NPP increase is quite uniform and statistically significant over most of throughout the entire basin and is equal approximately equal to $\pm 7\%$ in RCP4.5, which is approximately the half of the value more than twice that observed in the RCP8.5 (approximately 17%). Under the RCP8.5 emission scenario there is a 7% to -23% increase in NPP throughout the basin, with the relative local maxima observed mainly highest values in the coastal areas -observed of in the northwestern Western Mediterranean, Levantine basin, Northern Adriatic Sea, Gulf of Lion, Aegean Sea and Levantine basin (similar results, although with lower rates,

679 were found at the end of the 21st century by Solidoro et al., 2022+). Conversely, under the RCP4.5 scenario, the Adriatic
 680 Sea is still characterized by a negative and not significant anomaly (-1%), while for the rest of the basin the sign of the
 681 anomaly is positive and statistically significant, with the greatest values observed in the N~~orth~~westernWestern
 682 Mediterranean (approximately 12%, which is almost half of the variation observed in the RCP8.5 scenario). In both
 683 scenarios, there is still a negative anomaly in the Rhodes gyre area is observed, which is extremely weak in RCP8.5. Both
 684 negative anomalies are temporally consistent with some convective events taking place in both areas after 2080 and shown
 685 in Fig. S4.
 686

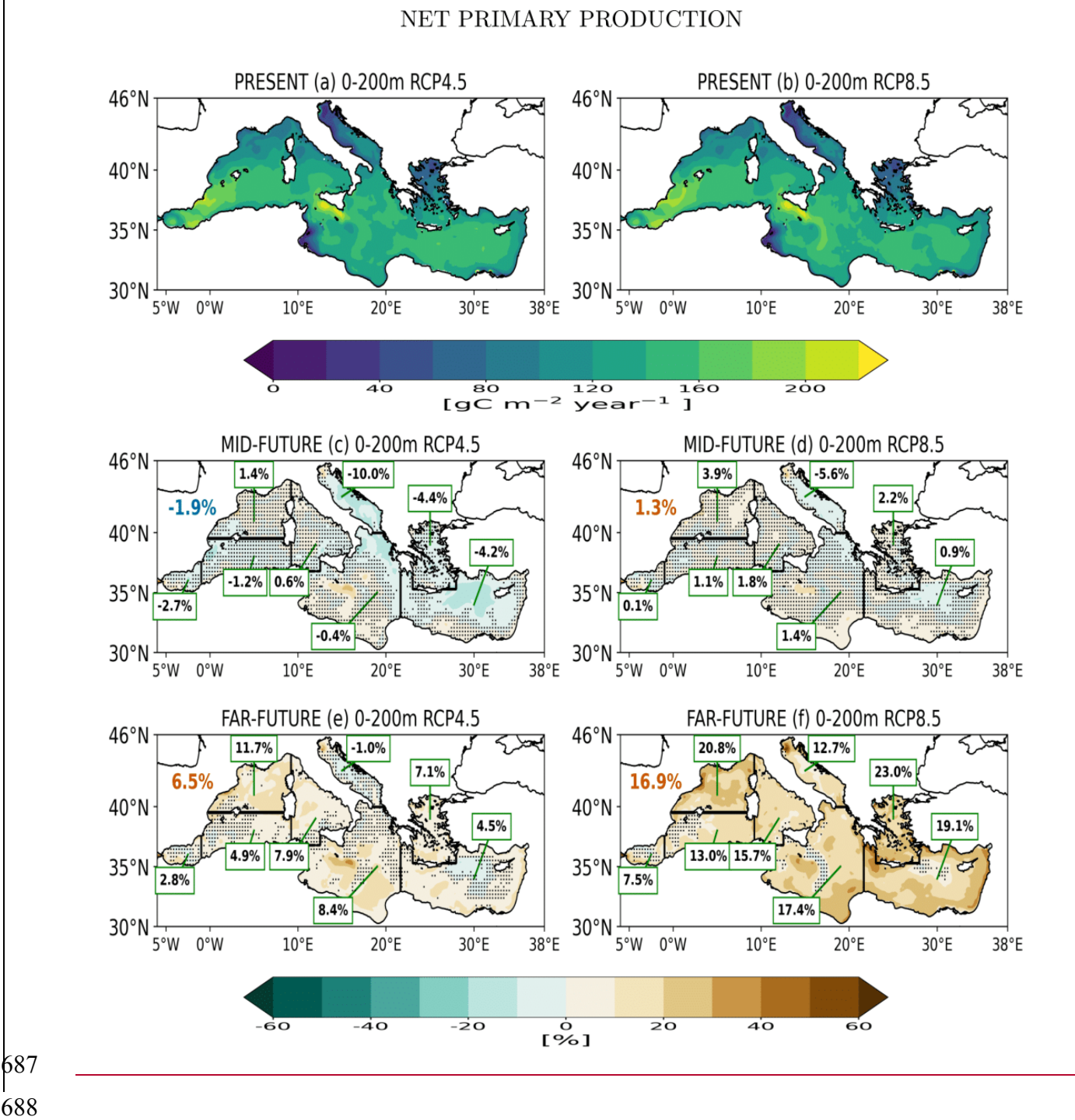


Fig. 11 - Integrated net primary production variation (in $\text{gC m}^{-2} \text{ year}^{-1}$) in first 0-200m in the PRESENT (2005-2020, a,b), and relative climate change signal (with respect to the PRESENT, in units of pH) in the MID-FUTURE (2040-2059, c,d) and FAR-FUTURE (2080-2099, e,f) in the RCP4.5 (left column) and RCP8.5 (right column) scenarios. The Mediterranean average relative climate change signal in each period (with respect to the PRESENT) is displayed by the top-left colored value (blue or dark orange when negative or positive). Values in the green boxes is the average relative climate change in each period and in each sub-basin shown in Figure 1. Domain grid points where the relative climate change signals are not statistically significant according to a Mann-Whitney test with $p < 0.05$ are marked by a dot.

As shown by Lazzari et al. (2014) and Solidoro et al. (2022+), the overall warming of the water column also results in an increase in community respiration. In agreement with that, Fig. S9 (see the supplementary materials) shows the spatial distribution of phytoplankton respiration (RESP) changes in the MID-FUTURE. It is possible to observe some differences with respect to NPP. In both scenarios, there is an overall decrease in the RESP with respect to the beginning of the 21st century, which is approximately equal to -24% in the RCP4.5 and -42% in the RCP8.5. In both scenarios the projected changes are again positive (and not statistically significant) signals can be observed in both scenarios in the Northern Adriatic, most of the coastal areas of the Northern Western Mediterranean, Central and Southern Ionian and coastal areas of parts of the Levantine basin. As previously observed for NPP, the Adriatic Sea has an overall negative and statistically significant anomaly, as well as together with the Northern Ionian Sea and the area of the Rhodes gyre. The Northwestern Western Mediterranean is the only area where the variation has an opposite sign in two scenarios: it is negative (-1.4%) in RCP4.5 and positive (approximately 1%) in RCP8.5. In both cases the projected changes are not significant.

In the FAR-FUTURE, the pattern of variation is coherent with that already observed in the NPP (Fig. 11). RESP increases at the end of the 21st century over the entire basin of approximately 54% (11%) in RCP4.5 (RCP8.5); again more than doubling the value observed in RCP4.5 (5%). Under the RCP4.5 scenario, the Adriatic Sea, with the northern part as the only exception, and the Rhodes gyre area are still characterized by a negative anomaly while under RCP8.5, the highest values are observed in the Northwestern Western Mediterranean (this is also true for the RCP4.5 scenario), Aegean Sea and Levantine basin. Under the RCP4.5 scenario, the Adriatic Sea, with the northern part as the only exception, is still characterized by a negative anomaly.

The overall increase in the respiration community and of the vertical stratification (which in turn affects the sinking velocity of the particles) has as a consequence on the decrease in the organic stock matter in the water column. The temporal evolution of the carbon organic matter standing stock for the 2005-2099 in RCP4.5 and RCP8.5 simulations between 0-100 m and 200-600 m in the whole Mediterranean and in its western Western and eastern Eastern basins is shown in Figure 12. The evolution behaviour of the carbon organic matter standing stock is similar to that observed in the dissolved nutrients, with a substantially stable signal in the first 30 years of the 21st century and a decrease after 2030. Afterwards, while RCP4.5 shows a recovery at the end of the 21st century, in particular, the projected decline in the RCP8.5 is projects a decline of approximately equal to 5 mgC m^{-3} until the end of the century, while RCP4.5 shows a similar behaviour, despite a recovery that is also present, in this case, at the end of the 21st century. The same dynamics is

observed in the intermediate layer, where the decline after the period 2030-2035 is approximately equal to 0.3 mgC m^{-3} for the carbon stock, with another slight recovery observed in RCP4.5 at the end of the century.

Similar dynamics are also observed for plankton (both phyto- and zoo-, Fig. 13), bacterial biomass and particulate organic matter in the euphotic layer (Fig. 14). In the RCP4.5 simulation for all these biogeochemical tracers, in general a recovery in the biomass is observed at the end of the 21st century and the projected changes are approximately 50% with respect to the RCP8.5 scenario where no recovery is found observed. In particular, the decrease of the phytoplankton (zooplankton) biomass is approximately 2 (1.5 mgC m^{-3}) and appears to be stronger in the eastern Eastern basin than in the western Western basin. Under RCP8.5 the bacterial biomass is projected to decrease at the basin scale by the end of the century by approximately 0.5 mgC m^{-3} , by 0.2 mgC m^{-3} in the western Western basin and by 0.6 mgC m^{-3} in the eastern Eastern basin. Finally, the decline in particulate organic matter is approximately 1.5 mgC m^{-3} at the basin scale, approximately 1 (2 mgC m^{-3}) in the western Western (Eastern) basin and approximately 2 mgC m^{-3} in the eastern Eastern basin. In the intermediate layer, the decline of the bacterial biomass in the entire basin is fairly uniform and continuous until the end of the 21st century, with a variation of approximately about 0.3 mgC m^{-3} with respect to the beginning of the century. For the same layer, particulate organic matter declines after the period 2030-2035 but successively the signal remains substantially stable and, in particular in the western Western basin, tends has a tendency to recover at the end of the century. In the RCP4.5 simulation for all these biogeochemical tracers, we observe a recovery in the biomass at the end of the century is simulated for all these biogeochemical tracers and the projected observed change is approximately 50% with respect to the RCP8.5 scenario.

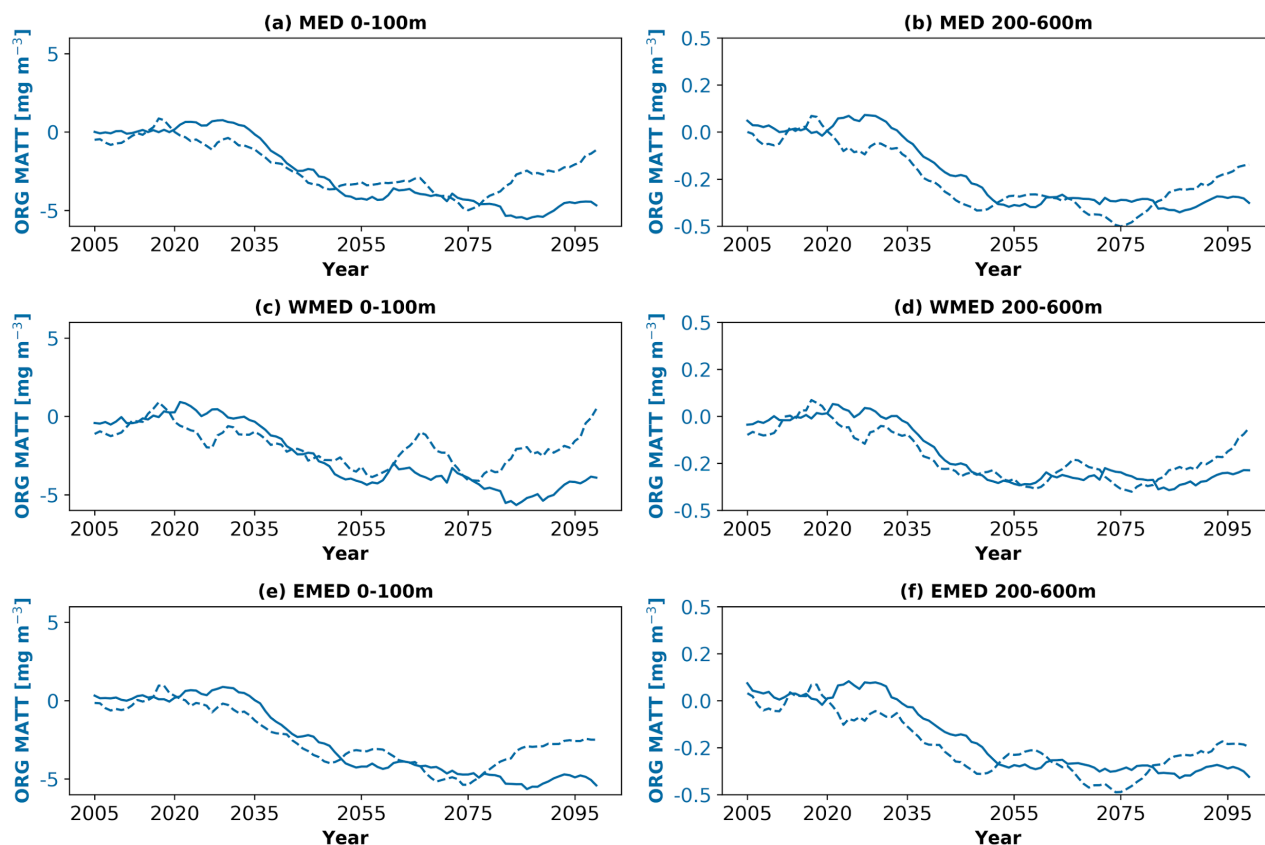


Fig. 12 - Yearly ~~timeseries~~time-series for the period 2005-2099 of Living/not Living organic Matter (in mg C m^{-3}) anomalies for the emission scenario RCP8.5 (solid line) and RCP4.5 (dashed line) in the Mediterranean Sea (MED, a-b), ~~Western~~Western Mediterranean (WMED, c-d) and ~~Eastern~~Eastern Mediterranean (EMED, e-f) for the layer 0-100_m (left column) and 200-600 m (right column) for the 2005-2099 period. The yearly ~~timeseries~~time-series have been smoothed using 10-years running mean.

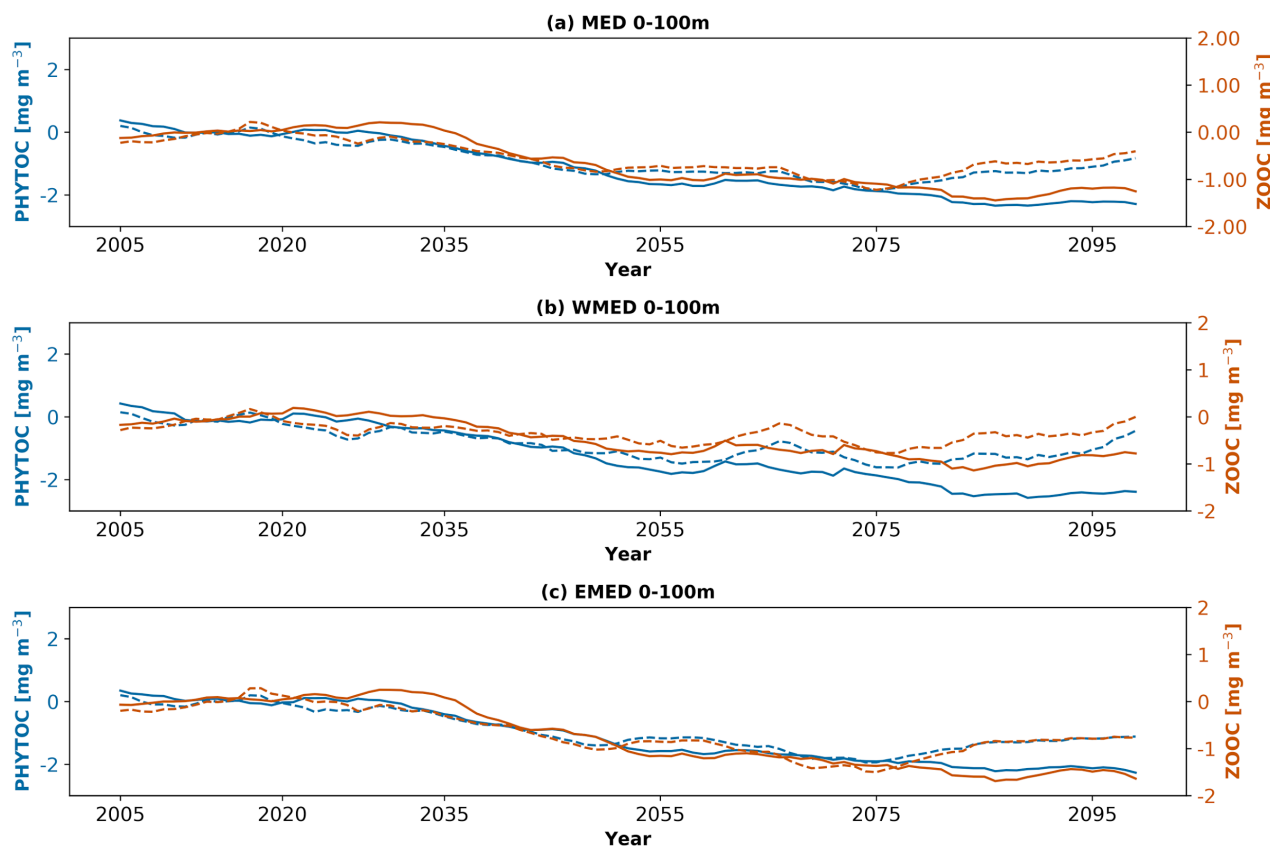


Fig. 13 - Yearly ~~timeseries~~time-series of Phytoplankton biomass (blue, in mg m^{-3}) and Zooplankton (dark orange, in mg m^{-3}) anomalies for the emission scenario RCP8.5 (solid line) and RCP4.5 (dashed line) in the Mediterranean Sea (MED, a), ~~Western~~Western Mediterranean (WMED, b) and ~~Eastern~~Eastern Mediterranean (c) for the layer 0-100_m and for the 2005-2099 period.

In the two scenarios, in both MID-~~FUTURE~~FUTURE and FAR-~~FUTURE~~FUTURE, the areas most affected by the statistically significant decline of phytoplankton (Fig. S10) and zooplankton (Fig. S11) biomasses are mainly the sub-basins of the easternEastern Mediterranean Sea, namely the Ionian Sea (mainly its Northern part), the Adriatic Sea (except for its Northern part), the Aegean Sea and the Levantine basin (in particular the Rhodes gyre area) and the Tyrrhenian Sea (only for the phytoplankton). Moreover, the negative anomaly in the area of Rhodes gyre is spatially coherent with the anomalies observed in gyre-is characterized by a permanent negative anomaly (as already observed in the case of NPP and RESP, consequences of the vertical convection phenomena in the area.) Conversely, positive but statistically signals signals for both variables can be observed only at the local scale in the Strait of Sicily and along the coast of the North~~hern~~ ~~Western~~Western Mediterranean (spatially coherent with the positive variations of the PO_4 discussed in section 3.3 and in

both cases not significant). For the latter, the zooplankton biomass in the North-Western Western Mediterranean increases by about 2% in the FAR-FUTUREFUTURE under emission scenario RCP4.5.

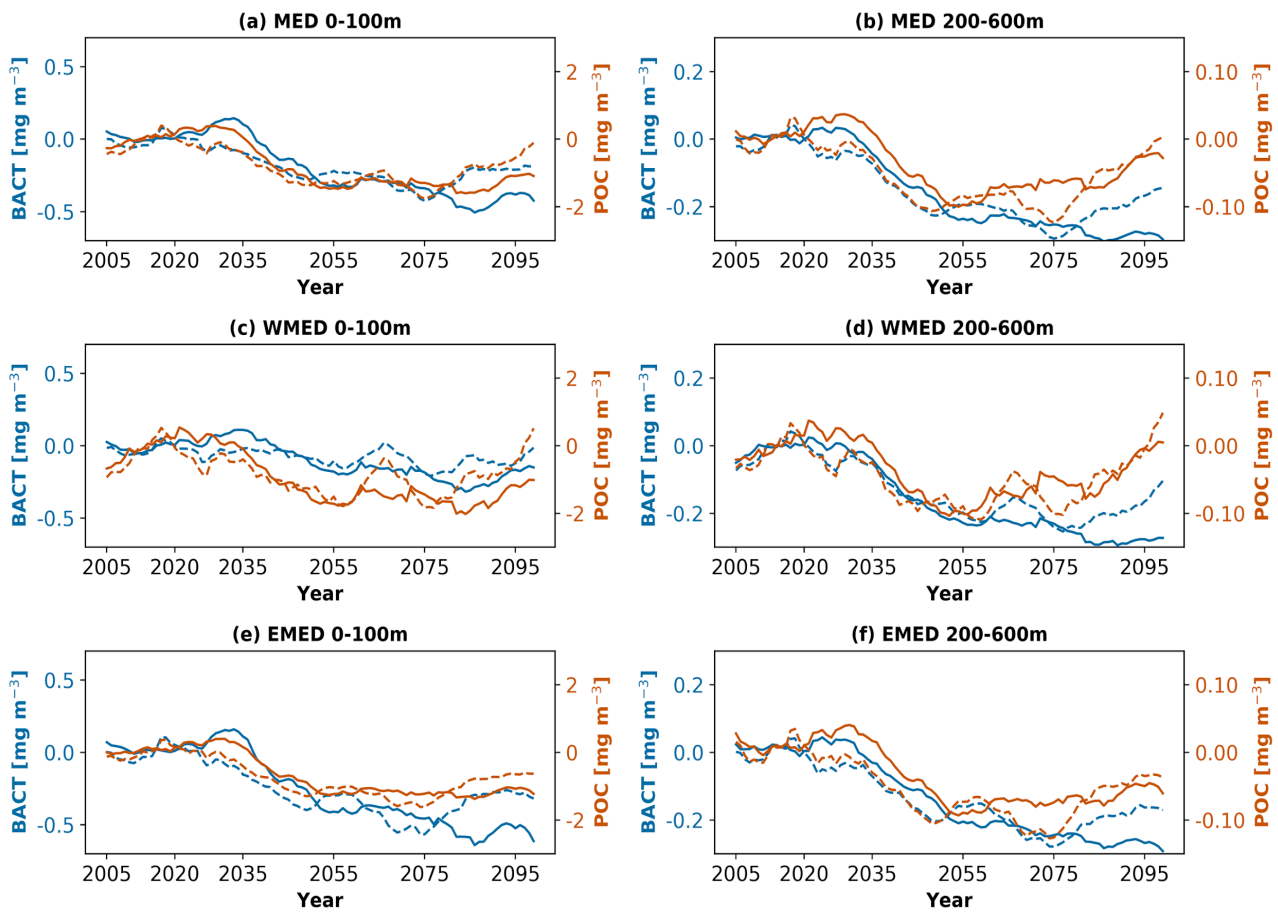


Fig.14- As Fig.8 but for bacterial biomass (blue, in mg m^{-3}) and particulate organic matter (dark orange, in mg m^{-3})

Also, in the case of bacterial biomass (Fig. S12) and particulate organic matter (Fig. S13) the decline along the 21st century will mostly affect the euphotic and the intermediate layers of the eastern Eastern basin, in both MID- and FAR-FUTUREFUTURE, with relative maxima observed in the Levantine basin (around 33.5 % in RCP4.5 and 50% in the RCP8.5 scenario). This decline is related to an increase of the respiration at community level, as observed for phytoplankton (Fig. S9). However, there are some exceptions to the general decline of the bacterial biomass and particulate organic matter in the basin. For example, in the Adriatic Sea, under scenario RCP8.5, the decrease of the bacterial biomass with respect to the beginning of the century is only 1% with a slight positive anomaly appearing in the southern Adriatic at the end of 21st century (not statistically significant, Fig. S12). In the case of particulate organic matter, the Strait of Sicily and the Northern Adriatic Sea are characterized by a permanent positive signal in both layers and scenarios as observed before for PO_4 —and also in this case not statistically significant. Moreover, in RCP4.5 simulation, in the FAR-FUTUREFUTURE period, the North-Western Western Mediterranean shows an increase of the particulate organic matter content in the euphotic and intermediate layers (here statistically significant in the area of the Gulf of Lion).

3.4 Spatial and temporal evolution of dissolved inorganic carbon (DIC) and pH

A basin-wide continuous increase in DIC is projected until the end of the 21st century, with a stronger signal observed in the RCP8.5 scenario (Fig. 15), and more specifically, in the [eastern](#) Eastern part of the Mediterranean basin. In fact, in the euphotic layer, the increase in DIC with respect to the beginning of the century is approximately $150 \mu\text{mol kg}^{-1}$ under RCP8.5 in the [eastern](#) Eastern basin, while it is approximately $120 \mu\text{mol kg}^{-1}$ in the [western](#) Western basin. Additionally, in the intermediate layer, DIC increases by approximately $120 \mu\text{mol kg}^{-1}$ with respect to the beginning of the century: this value is approximately the same for both the [western](#) Western and [eastern](#) Eastern basins and is double with respect to that observed in the RCP4.5 scenario.

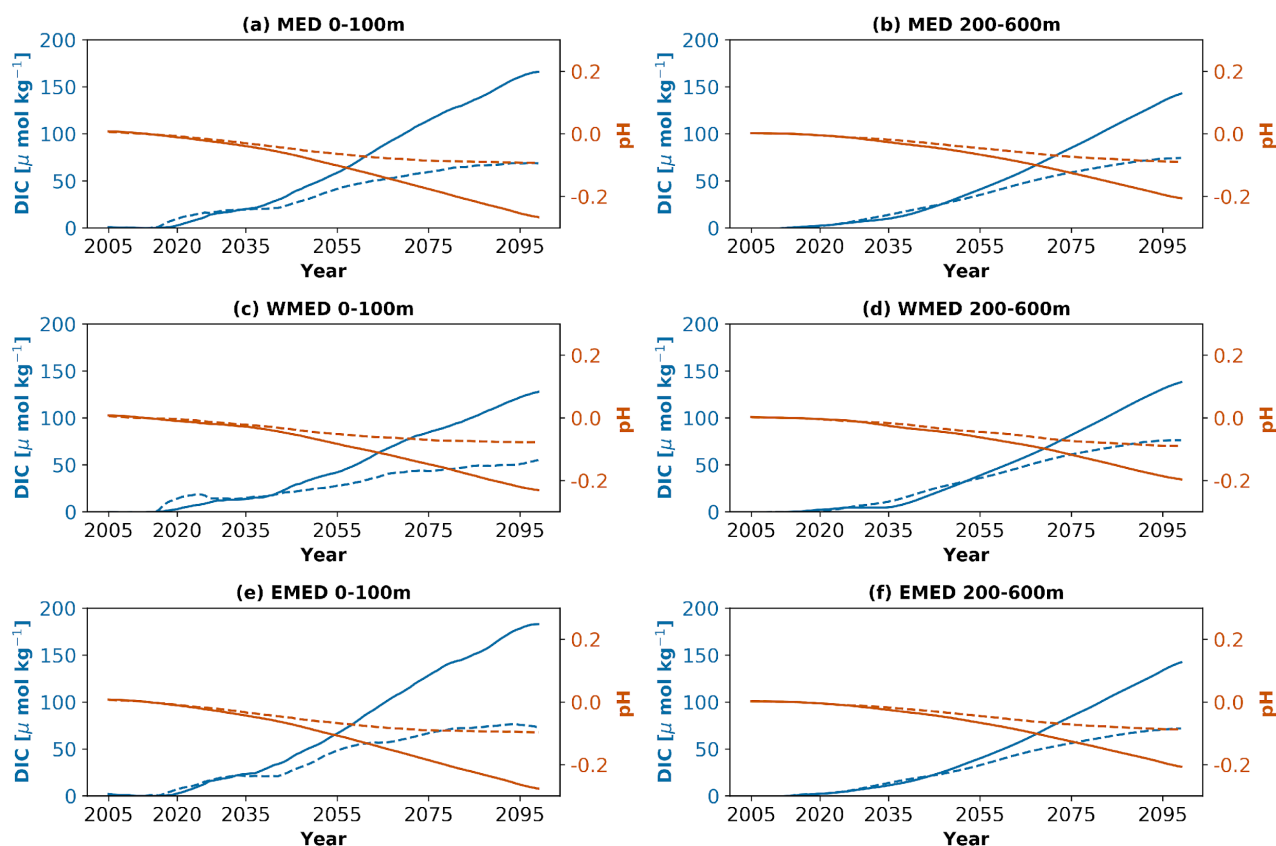


Fig. 15 - as Fig.14 but for Dissolved Inorganic Carbon (blue, in $\mu\text{mol kg}^{-1}$) and pH (dark orange)

Although community respiration can play a role in the increase in DIC, [in the Mediterranean region](#) a predominant mechanism is represented by the air-sea CO_2 exchange ([D'Ortenzio et al., 2008](#); [De Carlo et al., 2013](#); [Hassoun et al., 2019](#); [Wimart-Rousseau et al., 2020](#)). In fact, looking at the terms controlling the DIC increase, the air-sea CO_2 exchange shows an almost balanced condition in the present-day, [which is consistent with the 1999-2015 reanalysis](#) ([D'Ortenzio et al., 2008](#); [Melaku Canu et al., 2015](#)), and an increase throughout the 21st century as a consequence of the increase in atmospheric CO_2 (Fig. 16, a, [be](#)). The CO_2 flux increase is almost linear and is [equal](#) fairly in the two scenarios until 2050. Then, the RCP4.5 scenario shows [a](#) smoothing in the second half of the century, which is consistent [consistently](#) with [the](#) reduced atmospheric emissions, while the linear increase persists under RCP8.5 (Fig. 16, [ab, be](#)).

The two main Mediterranean sub-basins behave quite differently: the CO₂ air-sea sink is three times greater in the western Western part than in compared to the eastern Eastern part, reflecting the influence of both DIC and temperature spatial gradients (i.e., higher values of DIC and temperature in the eastern Eastern basin). In order to assess the temperature and DIC contributions Disentangling the temperature and DIC contributions to the pCO₂ temporal evolution, the carbonate system equations of the BFM model have been solved in offline mode, keeping constant, alternatively, temperature and DIC concentration. The increase in the temperature has been shown to evolution reveals that the impact of the increase in temperature on saturation accounts for 25% of the total increase in the pCO₂. The remaining part of the pCO₂ increase can be ascribed to the DIC concentration increase while the remaining part is due to the DIC concentration increase. In the western Western part, a less pronounced temperature effect (i.e., temperature \uparrow increases slower in the western Western part) causes an undersaturation condition of pCO₂ (i.e., pCO₂^{sea} lower than pCO₂^{atm} values) compared to the eastern Eastern conditions, triggering the much higher CO₂ absorption in the western Western Mediterranean.

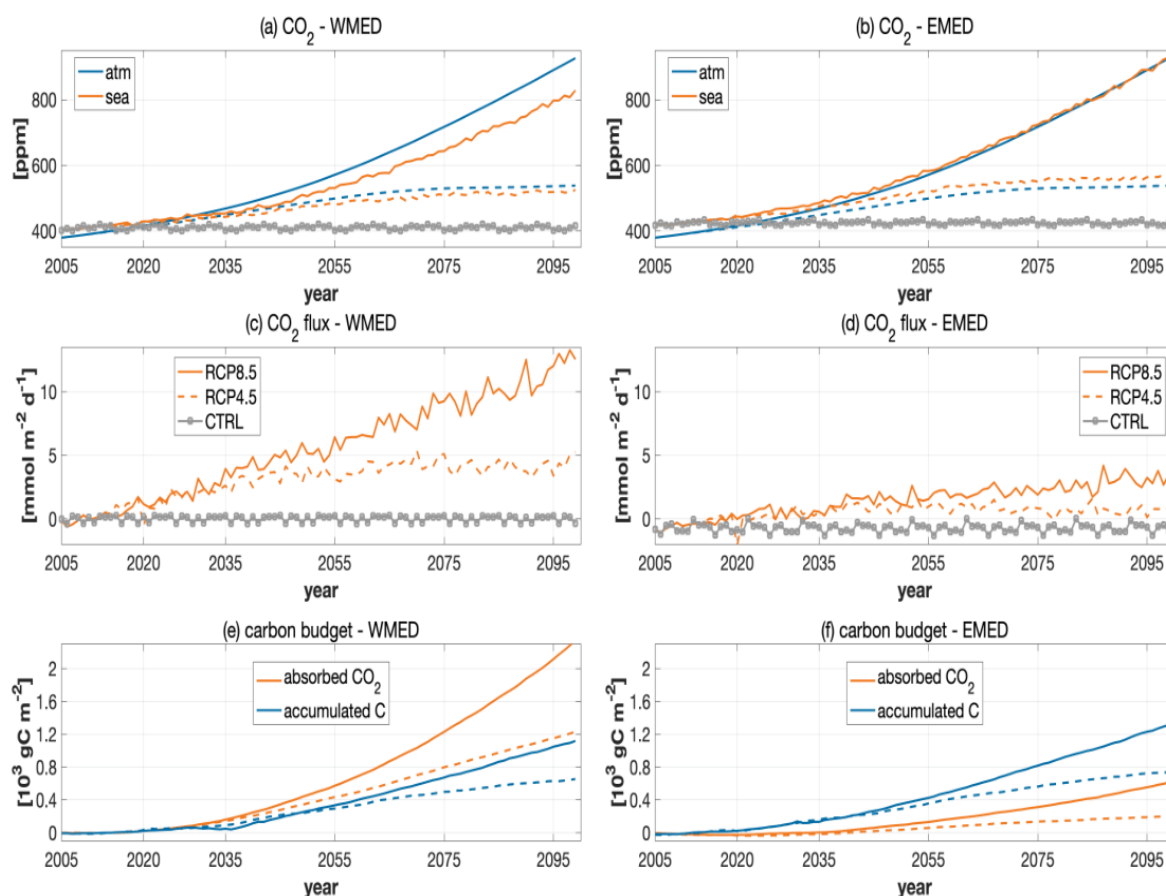


Fig.16 - Atmospheric and marine pCO₂ (a,b), CO₂ air-sea exchange (c,d) and cumulative CO₂ absorbed and accumulated in the water column (e,f) during the scenario simulations (e,f) in the western Western (a,c,e) and eastern Eastern (b,d,f) Mediterranean Sea. Two scenarios RCP4.5 (dashed line) and RCP8.5 (continuous line) and control simulation (CTRL, gray line) are reported.

As a result of the air-sea CO₂ sink, ~~for example~~ the RCP8.5 scenario shows a steady DIC accumulation after 2030 with values of ~~more than~~ 2 $\mu\text{mol kg}^{-1} \text{ year}^{-1}$ in the first 600 m (500 m) of the water column for the ~~western~~Western basin (~~eastern~~Eastern basin; Fig. 17).

The increase in DIC in the upper layer is approximately 1.5% and 2.5% in the ~~western~~Western and ~~eastern~~Eastern basins, respectively, in the MID-~~FUTURE~~FUTURE, and 5% and 7% in the FAR-~~FUTURE~~FUTURE (Fig.S14~~not shown~~). In the 200-600 m layers, the DIC increase follows the same pattern as that in the upper layer, but with smaller changes (i.e., approximately 1-2% less). Then, while the DIC increase does not impact the water column below 1200 m in the ~~western~~Western basin, DIC still accumulates until 2000 m in the ~~eastern~~Eastern basin at a rate of almost 0.5 $\mu\text{mol kg}^{-1} \text{ year}^{-1}$ (Fig. 17). Occasional events of deep transport of DIC can be recognized (e.g. around the years 2035, 2045, 2085 and 2095, similar to what observed in case of ~~the~~ oxygen in Fig.9) and the water column results enriched down to 1000-1500 m with a rate of approximately 1 $\mu\text{mol kg}^{-1} \text{ year}^{-1}$. In the surface layer (i.e., first 50-100 m), the interannual variability ~~of in~~ atmospheric conditions (i.e., specific annual wind and temperature seasonal cycles triggering the CO₂ fluxes) and ~~the~~ winter mixing produces an irregular succession of positive and negative annual changes, which can partially hide the long-term effect of the increase in atmospheric pCO₂. Thus, the cumulative sum of the CO₂ absorbed through air-sea exchanges and of the carbon accumulated in the water column (Fig. 16, ~~ee,f-panel~~) highlight the different ~~behavior~~behaviour of the two main sub-basins. The ~~western~~Western basin absorbs much more atmospheric CO₂ than the ~~eastern~~Eastern basin, with even larger differences in the RCP8.5 scenario. By the end of the RCP8.5 scenario, ~~we observe~~ 1.8 PgC of atmospheric CO₂ sink in the ~~western~~Western subbasin while only 1 PgC in the ~~eastern~~Eastern subbasin ~~are~~ ~~observed~~, consistent with ~~what~~ the estimates ~~of discussed in~~ Solidoro et al. (2022~~4~~).

However, the fate of the absorbed carbon is quite different: the ~~western~~Western basin ~~during the 21st century (RCP8.5 scenario)~~ accumulates only 0.85 PgC ~~by the end of RCP8.5~~, while 1.7 PgC are retained in the water column of the ~~eastern~~Eastern basin. As shown in Figure 16~~7~~ (lower panel) for the RCP8.5 scenario, the ~~eastern~~Eastern basin accumulates almost 2 moles of carbon for each atmospheric CO₂ mole absorbed (up to 3 in the RCP4.5), while it is less than 0.5 for the ~~western~~Western basin. The different efficiency is eventually triggered by the thermohaline circulation change: the ~~western~~Western Mediterranean carbon is partly exported to the ~~N~~orthern Atlantic Ocean, while an increased quota of carbon input from rivers and across the Sicily channel are retained in the ~~eastern~~Eastern basin together with the atmospheric CO₂ sink after the weakening of the thermohaline circulation (Fig.4). The RCP4.5 scenario shows similar dynamics to RCP8.5, with rates of CO₂ absorption (Fig. 16~~7~~) and of DIC accumulation almost halved, and the impact of the interannual variability on surface layer dynamics much more amplified (not shown). As a result, the total sequestered atmospheric CO₂ equals to 0.8 and 0.25 PgC in the ~~western~~Western and ~~eastern~~Eastern basins, while the increases of the carbon pool are 0.5 PgC and 0.9 PgC, respectively.

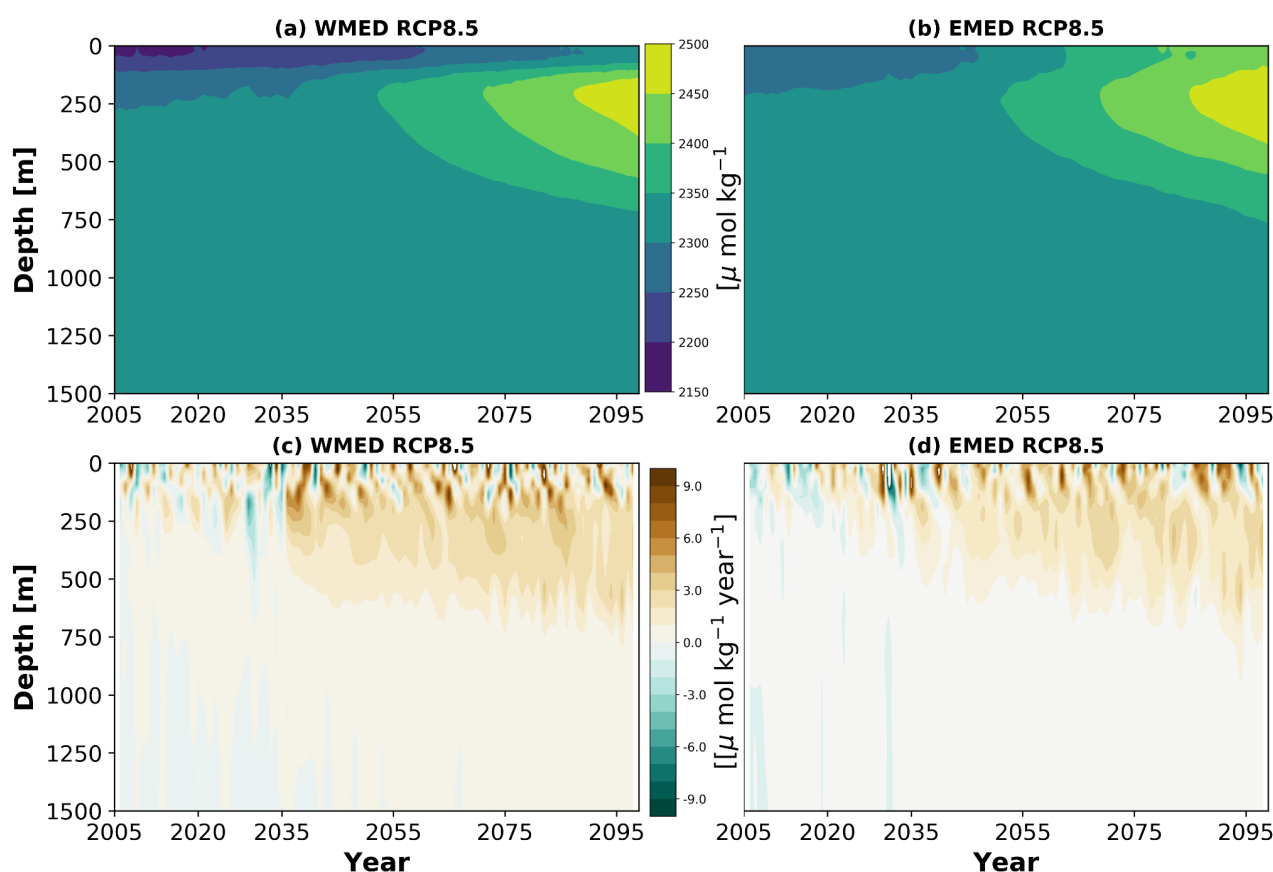


Fig. 17 - Hovmoeller diagram of DIC ($\mu\text{mol kg}^{-1}$, panel a,b) and annual rate of change of DIC ($\mu\text{mol kg}^{-1} \text{ year}^{-1}$, panel c,d) in the ~~western~~Western (a,c) and ~~eastern~~Eastern (b,d) Mediterranean Sea in RCP8.5 scenario.

Consequently, to the CO_2 invasion and DIC increase, the change in the carbonic acid equilibrium causes a generalized decrease in pH, as also shown in Solidoro et al. (2022+) in the case of the A2 scenario. The change in pH, which is statistically significant everywhere and very well anti-correlated in time and space with the DIC change (on the basin scale the correlation coefficient is lower than -0.90 with $p < 0.05$; Fig.S14 Fig.S14) and almost similar in both Western and Eastern Mediterranean (as already projected by Goyet et al, 2016), is approximately by the end of the century equal to 0.1 in the RCP4.5 and 0.25 units by the end of the century in the RCP8.5 scenario (Fig. 18), but some differences are visible among subbasins. The largest decreases in pH are projected in both scenarios in the upper layer of the North-Western Mediterranean, Tyrrhenian Sea, Adriatic Sea and Aegean Sea and in the 200-600 m layers of the Tyrrhenian Sea, Ionian Sea and Aegean Sea in the FAR-FUTUREFUTURE (Fig. 18). RCP4.5, which follows RCP8.5 evolution until the MID-FUTUREFUTURE period, presents a decrease in pH that does not exceed 1.1-1.2% in both the upper and 200-600 m layers by the end of the century.

pH

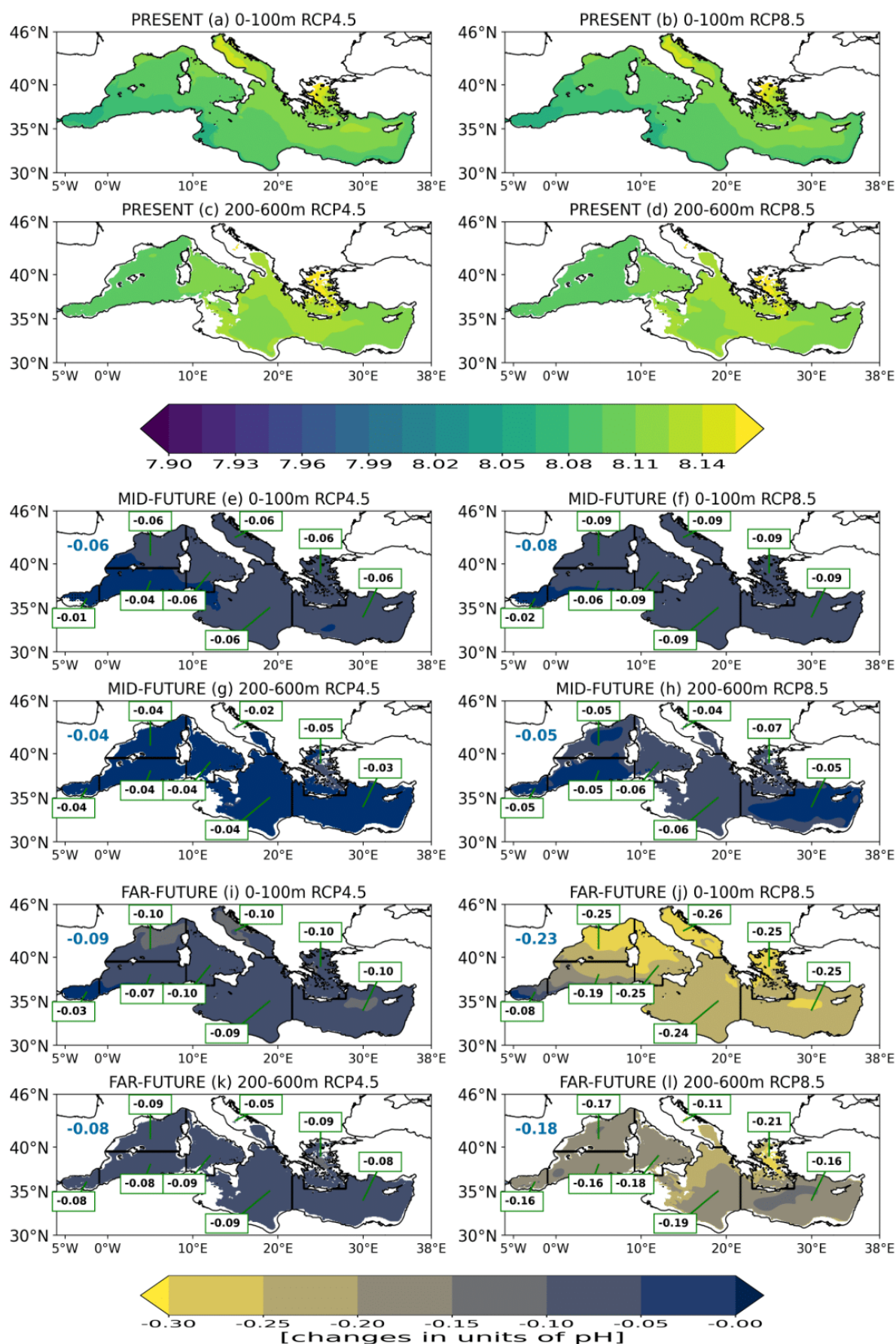


Fig. 18 –pH in the layers 0-100m and 200-600m in the PRESENT (2005-2020, a,b,c and d), and relative climate change signal (with respect to the PRESENT, in units of pH) in the MID-FUTURE (2040-2059, e,f,g and h) and FAR-FUTURE (2080-2099, i,j,k and l) in the RCP4.5 (left column) and RCP8.5 (right column) scenarios. The Mediterranean average relative climate change signal in each period (with respect to the PRESENT) is displayed by the top-left colored value (blue or dark orange when negative or positive). Values in the green boxes is the average relative climate change in each period and in each sub-basin shown in Figure 1. Domain grid points where the relative climate change signals are not statistically significant according to a Mann-Whitney test with $p < 0.05$ are marked by a dot.

4. Discussions and Conclusions

In this study, ~~we use~~ the coupled physical-biogeochemical model MFS16-OGSTM-BFM ~~is used~~ to simulate the biogeochemical dynamics of the Mediterranean Sea during the 21st century under the two emission scenarios RCP4.5 and RCP8.5, and to assess some climate-related impacts on the marine ecosystems of the basin.

~~To the best of the authors' knowledge this work is the first to focus on the Mediterranean Sea based on the projection of the biogeochemical tracers dynamics under two different emission scenarios and with horizontal and vertical resolutions (1/16° and 70 vertical levels) that are higher than those of previous works available in the scientific literature that focuses on the area (e.g Lazzari et al., 2014; Macias et al., 2015; Richon et al., 2019; Pagès et al., 2020; Solidoro et al., 2021). To the best of the authors' knowledge, this work is the first one that which analyzes long-term eddy-resolving projections of the biogeochemical dynamics of the Mediterranean Sea under two different emission scenarios. In fact, the horizontal and vertical resolution (1/16° and 70 vertical levels) of the long-term projections here analyzed is higher than that of previous works available in the scientific literature that focuses on the area (e.g Lazzari et al., 2014; Macias et al., 2015; Richon et al., 2019; Pagès et al., 2020; Solidoro et al., 2022). Moreover, the majority of the recent scientific works discussing the impacts of climate change on the biogeochemical dynamics of the Mediterranean Sea are based on the analysis of simulation that considered the worst-case emission scenario (A2 or RC8.5; Moullec et al., 2019; Richon et al., 2019; Pagès et al., 2020; Solidoro et al., 2022).~~

The use of eddy-resolving ~~higher- resolution horizontal~~ and ~~of a higher~~ vertical resolutions allows a more detailed representation of the vertical mixing and ocean convection processes, which play a fundamental role in the ventilation of the water column and in the nutrient supply into the euphotic layer of the basin (Kwiatkowski et al., 2020). ~~Moreover, the use of a 1/16° higher resolution for the projections horizontal resolution for the projections has allowed to resolve, identify and characterize, for the first time, spatial gradients, existing in the same sub-basins (such as in the Adriatic Sea) or between coastal and open ocean areas (such as in the North-Western Mediterranean). A more detailed representation of the spatial distribution of the projected changes and of their statistical significance that involve the signs and statistical significance of the projected changes for different certain biogeochemical tracers and properties. Moreover, the higher resolution. This represents an clear advantage for the future assessment of climate change impacts on specific organisms, habitats or target areas, also at sub-basin scale.~~

923 The analysis of the thermohaline properties and circulation of the Mediterranean Sea under emission scenarios RCP4.5
924 and RCP8.5 ~~found showed an overall~~ different levels of warming of the water column and ~~a~~-weakening of the
925 thermohaline circulation cell, with different parts of the basin being characterized by contrasting saltening and freshening
926 conditions as a function of the considered scenarios. Moreover, ~~we observe an overall~~ different levels of weakening of
927 the open ocean convection in the most important convective areas of the basin ~~are is~~ projected, with the only exception of
928 the Aegean Sea, where episodes of deep convection similar to the EMT could be observed at the end of the 21st century
929 (see also Adloff et al., 2015). All the projected changes are in agreement with those already depicted in recent model
930 studies (e.g. Somot et al., 2006; Adloff et al., 2015; Waldman et al., 2018; Soto-Navarro et al., 2020).

931
932 A comparison of the model outputs with available data in the present climate, together with previous studies performed
933 with the same model system, support the conclusion that the coupled model MFS16-OGSTM-BFM has a reasonably good
934 ability in reproducing the main biogeochemical features of the Mediterranean Sea and can be used as a tool for assessing
935 the future biogeochemical dynamics of the basin and its changes in response to climate change. The use of the bias-
936 removing protocol, is often advocated d as a good practice in climate studies, but rarely implemented in biogeochemical or
937 ecosystem projections (e.g. Solidoro et al., 2022⁺) and it, add further robustness to our results.

938
939 Our projections for the biogeochemical tracers and properties at the end of the 21st century shows
940 several signals (see ‡Table SP1 for a synthetic overview) that are mostly in agreement with previous
941 studies, at least with those based on the use of the worst-case emission scenarios. The magnitude of
942 the projected changes has been shown to be, in general, scenario-dependent with the largest deviations
943 from the present climate state observed in the RCP8.5 emission scenario (‡Table SP1). On the other
944 hand, the analysis of the projections under RCP4.5 found in most of the biogeochemical variables
945 (for example dissolved nutrients and biomasses) by the end of the 21st century a tendency to recover
946 the values observed in the present climate (‡Table SP1).

947
948 As shown in the previous sections, our simulations, by covering also the RCP4.5 scenario, highlight
949 how an intermediate greenhouse emission scenario produces results that are not simply an average
950 between the present condition and the RCP8.5, but (at least for some variables) something
951 quantitatively different. For example, the temporal evolution of pH (Fig.15) is similar in two
952 scenarios in the first 30 years of the 21st century. Conversely, after 2050, pH undergoes a substantial
953 decrease under RCP8.5 while it remains almost stable under RCP4.5 with a final projected variation
954 lower than the half with respect to the worst case scenario.

955
956 This supports the idea - possibly based on the existence of a certain buffer capacity and renewal rate
957 in a system like the Mediterranean Sea- that the implementation of policies of reducing CO2 emission

could be, indeed, effective and could contribute to the foundation of ocean sustainability science and policies.

The decline in the dissolved nutrients at the surface under RCP8.5 scenario is comparable with that observed in Richon et al. (2019). However, they ~~he latter~~ also projecting an overall increase in the concentration of both nutrients at the surface after 2050, which is ascribed by the authors to river and Gibraltar inputs that are not constant over time (as in our case) but are based on a global climate scenario simulation. As highlighted by Richon et al. (2019), the sensitivity of the biogeochemical fluxes at the river loads and Gibraltar exchanges is of paramount importance, and surely worthy of further investigation. Nevertheless, the increase in the concentration of nutrients in the intermediate layers of both the Western Mediterranean and Levantine basin can be also traced back to the reduced vertical mixing resulting from the increase in the vertical stratification (Somot et al., 2006; Adloff et al., 2015; Richon et al., 2019).

Different levels of increase in the net primary production and respiration are projected in both scenarios although many recent studies in the Mediterranean region have shown a different response of integrated net primary production to climate change in both Western and Eastern basins (e.g. Macias et al., 2015; Moullec et al., 2019; Pagès et al., 2020). In fact, this response may vary according to the sensitivity of the assumptions (model equations) for primary production and recycling processes to changes in temperature (Moullec et al., 2019). In the BFM model temperature regulates most of the metabolic rates with a Q10 formulation (Vichi et al., 2015). The increase in net primary production is a consequence of such dependence. In other studies (Eco3M-Med model; Pages et al., 2020) organisms are always optimally adapted and no temperature dependence is accounted for in the physiology. This different parameterization could be connected to the different results in terms of trends; in fact, the scenarios based on the Eco3M-Med model results in a reduction of net primary production. In this case surface nutrient reduction, rather than temperature, affects the net primary production trend producing a decrease. The relative impact of different drivers (nutrient supply versus organism's adaptation to average water temperature) could be explored with dedicated sensitivity experiments.

Our projections of net primary production and biomass dynamics show how different levels of warming of the water column and consequent stratification have a direct impact on the ecosystem functioning by increasing the metabolic rates. Similar to the results obtained in Lazzari et al. (2014) and Solidoro et al. (2022), the increase in metabolic rates augments both primary production and respiration, but with the net effect of reducing living and non-living particulate organic matter, as suggested from theoretical considerations in O'Connor et al. (2011). The decoupled formulation of carbon uptake and net growth in the BFM model induces a further mechanism related to how carbon is channeled in the food web. In fact, the decrease in biomass is partially compensated by an increase in dissolved organic matter production in the basin by the end of the century (Solidoro et al., 2022; results not shown here).

~~The projected~~ basin-wide deoxygenation tendencies are found in both scenarios and ~~iares~~ comparable to trends observed on the Mediterranean scale by Powley et al. (2018) and, under RCP8.5, on the global scale by CMIP6 simulations (Coupled Model Intercomparison Project Phase 6; Kwiatkowski et al., 2020) and on the Mediterranean scale by Powley et al. (2018). The ~~formerlatter~~, using a box model, found a decrease in the oxygen content of the intermediate

layer in the range of 2-9% as a consequence of different projected changes in the solubility (due to the temperature increase) and in the thermohaline circulation of the basin. Furthermore, ~~the projections-our results~~ show that, in both our scenarios, deoxygenation is higher in the Eastern than the Western basin, where the Atlantic boundary condition might have dumped the deoxygenation trend, and in several coastal areas such as the Northern Adriatic (until -25 mmol m^{-3}). As also observed by Powley et al. (2018), the main driver of deoxygenation is the change in solubility, whereas changes in the circulation (i.e., weakening of the thermohaline circulation) should not substantially affect deep ventilation, and it is unlikely, even in the worst-case scenario, to reach hypoxia conditions in the deep layer of the basin by the end of the century. On the other hand, the greatest threat for considering the oxygen water content might be linked to the combination of surface warming and faster respiration processes in the coastal areas of the basin which could result in lower oxygen conditions and, thus, alteration of the local marine ecosystem functioning and structures (Bindoff et al., 2019~~5~~).

An increase in the dissolved inorganic carbon content and acidity of the water column (Solidoro et al., 2022) is found in both scenarios. The overall accumulation of CO_2 in the basin resulted in an acidification of the Mediterranean water with a decrease in pH of approximately 0.23 units in the worst-case scenario, which is slightly lower than the 0.3 projected on a global scale (Kwiatkowski et al., 2020) and lower than the value provided in Goyet et al. (2016), who projected, using thermodynamic equations of the CO_2 /carbonate system chemical equilibrium in seawater, a variation of 0.45 pH units in the basin under the worst SRES case scenario (and 0.25 pH units in the most optimistic SRES scenario). However, this last estimate probably tends to overestimate the future acidification of the basin, as it does not consider the decrease in the exchanges and the penetration of CO_2 across the ocean-atmosphere interface due to the warming of the water column (MedECC, 2020).

This difference in the response to climate change between the Western and Eastern basins has been also observed for the dissolved inorganic carbon accumulation and reflects indeed different factors such as the different ventilation and residence time of water masses in the two basins as well as the exchanges in the ~~Strait of Gibraltar~~ Gibraltar Strait (e.g. Alvarez et al., 2014; Stöven and Tanhua, 2014; Cardin et al., 2015; Hassoun et al., 2019). Results show that, in both scenarios, the Western basin, while adsorbing greater quantities, accumulates only a half of the atmospheric carbon stored by the Eastern basin (~~1.85 PgC~~) because in the former the carbon is partly exported to the Northern Atlantic Ocean, while in the latter, it is also affected by a more intense reduction of the thermohaline circulation and therefore in the vertical transport processes, the carbon is retained together with the atmospheric CO_2 sink. Additionally, in our case, the use of a high resolution for the biogeochemical projections has allowed to show that in many coastal areas the observed acidification is lower by approximately 8% with respect to the open ocean due to damping effects of alkalinity input from the rivers (not shown here).

The decrease in dissolved nutrients in the euphotic layer of the basin and in the intermediate layer of the central part of the Mediterranean Sea, the increases in the net primary production and respiration, the decline of the stocks of particulate carbon biomass (including phytoplankton, zooplankton, bacterial biomass and particulate organic matter), the uniform surface and subsurface deoxygenation of the water column simulated in the RCP8.5 scenario, are globally in agreement with the conclusions of previous regional and global case studies (e.g. Hermann et al., 2014; Lazzari et al., 2014; Macias

et al., 2015; Moullec et al., 2019; Richon et al., 2019; Pagès et al., 2020; Kwiatkowski et al., 2020; Solidoro et al., 2021). We also observe an increase in the dissolved inorganic carbon content and acidity of the water column (Solidoro et al., 2021).

The decline in many biogeochemical ~~tracer~~tracers and properties in the euphotic layer begins in the 2030-2035 period, in correspondence to the weakening of the thermohaline circulation in the basin (Fig. 4), and it is particularly marked in the ~~eastern~~Eastern basin. This shows that the modification of the circulation resulting from future climate scenarios has substantial effects on the biogeochemical properties of the basin. Changes in the thermohaline circulation of the basin also explain the increase in the nutrient concentration in the intermediate layer of the Levantine basin, which is a result of the weakening of the westward transport of nutrients through the Strait of Sicily (Fig.S5). ~~Nevertheless, the increase in the concentration of nutrients in the intermediate layers of both the western and Levantine basins can be also traced back to the reduced vertical mixing resulting from the increase in the vertical stratification (Somot et al., 2006; Adloff et al., 2015; Richon et al., 2019). The decline in the dissolved nutrients at the surface is comparable with that observed in Richon et al. (2019), the latter also projecting an overall increase in the concentration of both nutrients at the surface after 2050, which is ascribed by the authors to river and Gibraltar inputs that are not constant over time (as in our case) but are based on a global climate scenario simulation. As highlighted by Richon et al. (2019), the sensitivity of the biogeochemical fluxes at the river loads and Gibraltar exchanges is of paramount importance, and surely worthy of further investigation.~~

~~As already discussed in the introduction, many recent studies in the Mediterranean region have shown a different response of integrated net primary production to climate change. In fact, this response may vary according to the sensitivity of the assumptions (model equations) for primary production and recycling processes to changes in temperature (Moullec et al., 2019). Our projections of primary productivity and biomass dynamics show how the warming of the water column and consequent stratification have a direct impact on the ecosystem functioning by increasing the metabolic rates. Similar to the results obtained in Lazzari et al. (2014) and Solidoro et al. (2021), the increase in metabolic rates augments both primary productivity and respiration, but with the net effect of reducing living and nonliving particulate organic matter, as suggested from theoretical considerations in O'Connor et al. (2011). The decoupled formulation of carbon uptake and net growth in the BFM model induces a further mechanism related to how carbon is channelled in the food web. In fact, the decrease in biomass is partially compensated by an increase in dissolved organic matter production in the basin by the end of the century (Solidoro et al., 2021; results not shown here).~~

~~Surface and intermediate layer deoxygenation, which are driven by the projected warming and by the increase in the respiration and reduced oxygen inflow in the Gibraltar Strait, is rather uniform throughout the basin (approximately 15 mmol m⁻³ in the worst scenario at the end of 21st century), showing that in this case, the climate forcing acts almost uniformly over the Mediterranean Sea. Our basin-wide deoxygenation is comparable to trends observed on the global scale CMIP6 simulations (Kwiatkowski et al., 2020) and on the Mediterranean scale by Powley et al. (2018). The latter, using a box model, found a decrease in the oxygen content of the intermediate layer in the range of 2-9% as a consequence of different projected changes in the solubility (due to the temperature increase) and in the thermohaline circulation of the basin. Furthermore, our results show that deoxygenation is higher in the eastern than the western basin, where the Atlantic boundary condition might have dumped the deoxygenation trend, and in several coastal areas such as the~~

Northern Adriatic (until 25 mmol m^{-3}). As also observed by Powley et al. (2018), the main driver of deoxygenation is the change in solubility, whereas changes in the circulation (i.e., weakening of the thermohaline circulation) should not substantially affect deep ventilation, and it is unlikely to reach hypoxia conditions in the deep layer of the basin by the end of the century. On the other hand, the greatest threat considering the oxygen water content might be linked to local conditions of surface warming (such as in coastal areas).

This difference in the response to climate change between the western and eastern basins has been also observed for the dissolved inorganic carbon accumulation and indeed reflects the influence of the exchanges in the Gibraltar Strait. Results show that the western basin, while adsorbing greater quantities, accumulates only a half of the atmospheric carbon stored by the eastern basin (1.85 PgC) because in the former the carbon is partly exported to the northern Atlantic Ocean, while in the latter, it is also affected by a more intense reduction of the thermohaline circulation and therefore in the vertical transport processes, the carbon is retained together with the atmospheric CO_2 sink. The overall accumulation of the CO_2 in the basin resulted in an acidification of the Mediterranean water with a decrease of pH of approximately 0.25 units, which is slightly lower than the value (0.3) projected on a global scale (Kwiatkowski et al., 2020). Additionally, in our case, the use of a high resolution for the biogeochemical projections has shown that in many coastal areas the observed acidification is lower by approximately 8% with respect to the open ocean due to damping effects of alkalinity input from the rivers (not shown here).

Similar to all previous modelling cited studies (e.g Lazzari et al., 2014; Macias et al., 2018; Richon et al., 2019; Pagès et al., 2020), some sources of uncertainties for our projections need to be considered. As discussed before, MFS16 adequately reproduces the distribution of key physical properties and the thermohaline circulation of the basin. On the other hand, recent studies based on multi-model ensembles (Adloff et al., 2015; Richon et al., 2019; Soto-Navarro et al., 2020) have suggested that atmospheric forcing and boundary conditions can strongly affect the dynamics of the basin, particularly the vertical mixing, which plays a primary role in the distribution of nutrients in the euphotic layer, therefore affecting the dynamics of low trophic levels. Additional sources of uncertainties in the modelling framework can be traced back to the BFM biogeochemical model. For instance, in the present climate the model tends to clearly overestimate the chlorophyll-*a* at the surface and, even more, the oxygen concentration below 200 m (section 3.1). These overestimations can be propagated by the integration into the future projections. However, the conclusions of the present work should not be significantly affected by that because, at the same time, the CTRL simulation is also removed from both the scenario simulations. Moreover, the signs of the projected changes (not their absolute values) result from different physical and biogeochemical processes (e.g., temperature and respiration increase, weakening of the thermohaline circulation, increase in the stratification and so on) which are linked to the climate forcing and are independent from model uncertainties the biases that generate the biases discussed in section 3.1.

Furthermore, the set-up of the boundary conditions, namely the atmospheric deposition at the surface, the rivers nutrient loads and the vertical profiles in the Atlantic boundary can be very critical, especially in the land-locked Mediterranean basin. Atmospheric deposition is an important source of nutrients for the basin and it has been shown that the

biogeochemical dynamics of the Mediterranean Sea is influenced by aerosol deposition (e.g. Richon et al., 2018, 2019), especially during periods of stratification. The projected lower nutrient supply from sub-surface waters caused by climate-driven stronger stratification, ~~could~~^{will} likely increase the importance of the atmospheric deposition as a source of nutrients for the euphotic layer (Gazeau et al., 2021). Thus, possible future changes in the deposition of aerosols could influence the biogeochemistry of the basin and the nutrients concentration at the surface as projected for the 21st century and depicted in Section 3.3. However, ~~In fact, in in~~ both RCP4.5 and RCP8.5 simulations, ~~we used a~~ present-day phosphate and nitrogen deposition ~~is used, but~~ potential improvements ~~will~~^{could} be achieved ~~indeed~~ by the inclusion of more accurate deposition information derived from CMIP6 global estimates for the 21st century (O'Neill et al., 2016). ~~Moreover, the biogeochemical dynamics of the Mediterranean Sea is influenced by aerosol deposition (e.g. Richon et al., 2018, 2019), and thus, possible future changes in the deposition of aerosols could influence the biogeochemistry of the basin and the nutrients concentration at the surface projected for the 21st century and depicted in Section 3.3.~~

Similarly, the lack of river nutrient load projections under the prescribed emission scenarios can affect the projected nutrient budget of the Mediterranean basin. ~~We used Aa~~ climatology derived from the Perseus project (see Section 2.3) ~~is here adopted~~, which is, to our knowledge, the most reliable information. Indeed, it is reasonable to assume that land-use and runoff changes might impact future nutrient loads, although the magnitude and even the sign are presently unknown. Our river runoff was based on projections (Gualdi et al., 2013; Section 2.1) which estimated an average decrease by the end of the 21st century. Thus, the increase of nutrients observed in Fig. 9 and Fig. 10 in the Northern Adriatic and several coastal areas of the ~~western~~^{Western} basin can be partially related to the mismatch between a constant nutrient load and a decreasing runoff. However, it might worth to remember that the amount of nutrients entering the basin through its boundaries ultimately depends on the economic policies and land used/coverage scenarios and therefore they may be intrinsically subjective.

With DIC as the only exception, for the 21st century, ~~we used a~~ single vertical profile based on the present-day condition data ~~is used~~ and no future evolutions are considered for the boundary conditions at the Gibraltar Strait. If this approach allows to point out the effects of the changes in the basin circulation on the nutrient budgets, it could miss the influence on nutrients or other biogeochemical properties of a possible different future evolution of the exchanges in the ~~Strait of Gibraltar~~^{Gibraltar Strait} due to changes in the tracer concentrations in the Atlantic Ocean. ~~Moreover, the use of the same Atlantic boundary conditions for the two scenarios (section 2.3) could have led to an underestimation of a potential difference between the two scenarios in the areas most influenced by the Atlantic boundary (e.g. Alboran Sea and Southern Western Mediterranean).~~ Recent physical simulations have shown an increase of 3.7% in the surface flow at the Gibraltar Strait, which could imply an increase in the inflow of nutrients in the surface layer at ~~Strait of Gibraltar~~^{Gibraltar Strait} (Richon et al., 2019; Pagès et al., 2020), thereby eventually damping the decrease in the nutrient concentration at the surface projected for the 21st century. As previously observed, this could explain the observed differences among different studies that analysed future-projections of the biogeochemistry of the basin.

To conclude, ~~we demonstrated that~~ the methodology and results here presented, provide a robust picture of the evolution of the Mediterranean Sea biogeochemistry for the 21st century. Clearly, the new generation of Regional Earth System Coupled Models (RESM), with eddy-resolving ocean models such ~~as~~ the one exploited here, may partially reduce the limitations of using external (and possibly misaligned) sources of information for atmospheric and land input to the ocean.

1153 Indeed, by directly resolving the coupling between the Mediterranean Sea, the regional atmospheric domain and the
1154 hydrological component, a regional earth system coupled model (e.g., as in Sitz et al., 2017, and Reale et al., 2020a)
1155 allows the simulation of the different components of the climate system at the local scale, including aerosol and river
1156 loads.

1157

1158 **Acknowledgements**

1159 M. Reale has been supported in this work by OGS and CINECA under HPC-TRES award number 2015-07 and by the
1160 project FAIRSEA (Fisheries in the Adriatic Region - a Shared Ecosystem. Approach) funded by the 2014 - 2020 Interreg
1161 V-A Italy - Croatia CBC Programme (Standard project ID 10046951). This work has been partially supported by the
1162 Italian PRIN project ICC3 (Impact of Climate Change on the biogeochemistry of Contaminants in the Mediterranean
1163 Sea). ~~We acknowledge~~ the CINECA consortium is acknowledged for providing the computational resources through
1164 the IscraB project “Scenarios for the Mediterranean Sea biogeochemistry in the 21st century” (MED21BIO) and the
1165 IscraC DYBIO, EMED18 and MEDCLI16. This study has been conducted also using E.U. Copernicus Marine Service
1166 Information

1167

1168 **Data availability**

1169 Data produced in the numerical experiments are available through the portal dds.cmcc.it for both physical
1170 (<https://dds.cmcc.it/#/dataset/medsea-cmip5-projections-physics>) and biogeochemical
1171 (<https://dds.cmcc.it/#/dataset/medsea-cmip5-projections-biogeochemistry>) components.

1172

1173 **Author contribution**

1174 GC, PL, SS, MR and CS conceived the study. They designed the experiments together with TL ~~and MR~~. MR, GB and
1175 TL performed the numerical simulations. MR, GC, SS, TL and PL performed the analysis of the simulation results. MR
1176 prepared the first draft of the manuscript under the supervision of SS, GC, PL and CS and with the contribution from all
1177 the authors. All the authors discussed the results and contributed to the revision of the manuscript.

1178

1179 **Competing interest**

1180 The authors declare that they have no competing interests.

1181

1182 **References**

1183

1184 Álvarez, M., Sanleón-Bartolomé, H., Tanhua, T., Mintrop, L., Luchetta, A., Cantoni, C., Schroeder, K., and Civitarese,
1185 G.: The CO₂ system in the Mediterranean Sea: a basin wide perspective, Ocean Sci., 10, 69–92, [https://doi.org/10.5194/os-](https://doi.org/10.5194/os-10-69-2014)
1186 [10-69-2014](https://doi.org/10.5194/os-10-69-2014), 2014.

1187

1188 Adloff, F., Somot, S., Sevault, F., Jordà, G., Aznar, R., Déqué, M., Herrmann, M., Marcos, M., Dubois, C., Padorno, E.,
1189 Alcarez-Fanjul, E., Gomis, D., et al.: Mediterranean Sea response to climate change in an ensemble of twenty first century
1190 scenarios. *Clim Dyn* 45, 2775–2802. <https://doi.org/10.1007/s00382-015-2507-3>, 2015

1191
1192
1193
1194
1195
1196
1197
1198
1199
1200
1201
1202
1203
1204
1205
1206
1207
1208

1209
1210
1211
1212
1213
1214
1215
1216

1217
1218
1219
1220
1221
1222
1223
1224

Auger, P.A., Ulses, C., Estournel, C., Stemman, L., Somot, S. and Diaz, F.: Interannual control of plankton ecosystem in a deep convection area as inferred from a 30-year 3D modeling study: winter mixing and prey/predator in the NW Mediterranean. *Progress in Oceanography*, 124, 12-27, DOI: 10.1016/j.pocean.2014.04.004, 2014

[Benedetti, F., Guilhaumon, F., Adloff, F. and Ayata, S.D: Investigating uncertainties in zooplankton composition shifts under climate change scenarios in the Mediterranean Sea. *Ecography*, 41: 345-360. <https://doi.org/10.1111/ecog.02434>, 2018](#)

Bethoux, J. P., Morin, P., Chaumery, C., Connan, O., Gentili, B., and Ruiz-Pino, D.: Nutrients in the Mediterranean Sea, mass balance and statistical analysis of concentrations with respect to environmental change, *Mar. Chem.*, 63, 155–169, 1998

[Bindoff, N.L., Cheung, W.W.L., Kairo, J.G., Arístegui, J., Guinder, V.A., Hallberg, R., Hilmi, N., Jiao, N., Karim, M.S., Levin, L., O'Donoghue, S., Purca Cuicapusa, S.R., Rinkevich, B., Suga, T., Tagliabue, A., and Williamson, P.: Changing Ocean, Marine Ecosystems, and Dependent Communities. In: *IPCC Special Report on the Ocean and Cryosphere in a Changing Climate* \[H.-O. Pörtner, D.C. Roberts, V. Masson-Delmotte, P. Zhai, M. Tignor, E. Poloczanska, K. Mintenbeck, A. Alegría, M. Nicolai, A. Okem, J. Petzold, B. Rama, N.M. Weyer \(eds.\)\], 477-587, 2019](#)

Buga, L., ~~G. Sarbu, G., L. Fryberg, L., W. Magnus, W., K. Wesslander, K., J. Gatti, J., D. Leroy, D., S. Iona, S., M. Larsen, M., J. Koefoed Rømer, J., A.K. Østrem, A.K., M. Lipizer, M., A. Giorgetti, A.~~: EMODnet Thematic Lot n° 4/SI2.749773 EMODnet Chemistry Eutrophication and Acidity aggregated datasets v2018 doi: 10.6092/EC8207EF-ED81-4EE5-BF48-E26FF16BF02E, 2018

Butenschön, M., Lovato, T., Masina, S., Caserini, S., and Grosso, M.: Alkalinization Scenarios in the Mediterranean Sea for Efficient Removal of Atmospheric CO₂ and the Mitigation of Ocean Acidification. *Frontiers in Climate*, 3, 14. 2021

Canu, D. M., Ghermandi, A., Nunes, P. A., Lazzari, P., Cossarini, G., and Solidoro, C.: Estimating the value of carbon sequestration ecosystem services in the Mediterranean Sea: An ecological economics approach. *Global Environmental Change*, 32, 87-95. 2015

[Cardin, V., Civitarese, G., Hainbucher, D., Bensi, M., and Rubino, A.: Thermohaline properties in the Eastern Mediterranean in the last three decades: is the basin returning to the pre-EMT situation?, *Ocean Sci.*, 11, 53–66, <https://doi.org/10.5194/os-11-53-2015>, 2015.](#)

1225 Claustre, H., Morel, A., Hooker, S. B., Babin, M., Antoine, D., Oubelkheir, K., Bricaud, A., Leblanc, K., Quéguiner, B.,
 1226 Maritorena, S.: Is desert dust making oligotrophic waters greener? *Geophys. Res. Lett.*, 29, 1–4,
 1227 <https://doi.org/10.1029/2001GL014056>, 2002

1228 Colella, S., Falcini, F., Rinaldi, E., Sammartino, M., and Santoleri, R.: Mediterranean Ocean colour chlorophyll trends.
 1229 *PLoS ONE*, 11(6), e0155756. <https://doi.org/10.1371/journal.pone.0155756>, 2016

1230 Cossarini G., Lazzari P., Solidoro C.: Spatiotemporal variability of alkalinity in the Mediterranean Sea, *Biogeosciences*,
 1231 12, 1647-1658, <https://doi.org/10.5194/bg-12-1647-2015>, 2015

1232
 1233 [Cossarini G, Feudale L, Teruzzi A, Bolzon G, Coidessa G, Solidoro C, Di Biagio V, Amadio C, Lazzari P, Brosich A and](#)
 1234 [Salon S \(2021\) High-Resolution Reanalysis of the Mediterranean Sea Biogeochemistry \(1999–2019\). Front. Mar. Sci.](#)
 1235 [8:741486. doi: 10.3389/fmars.2021.741486](#)
 1236

1237 Crise A., Allen J., Baretta J., Crispi G., Mosetti R., Solidoro C.: The Mediterranean pelagic ecosystem response to
 1238 physical forcing *Progress in Oceanography* 44 (1-3), 219-243., 1999

1239
 1240 Crispi G., Mosetti R., Solidoro C., Crise A.: Nutrient cycling in Mediterranean basins: the role of the biological pump
 1241 in the trophic regime *Ecol. Model.*, 138pp.101-114, 2001

1242
 1243 Darmaraki, S., Somot, S., Sevault, F., [Nabat P., Cabos Narvaez W.D., Cavicchia L., Djurdjevic V., Li L, Sannino G.,](#)
 1244 [Sein D.Vet al.](#): Future evolution of Marine Heatwaves in the Mediterranean Sea. *Clim Dyn* **53**, 1371–1392.
 1245 <https://doi.org/10.1007/s00382-019-04661-z>, 2019

1246
 1247 [De Carlo, E.H., Mousseau, L., Passafiume, O., Drupp, P., Gattuso, J.P.: Carbonate Chemistry and Air–Sea CO₂ Flux in a](#)
 1248 [NW Mediterranean Bay Over a Four-Year Period: 2007–2011. *Aquat Geochem* **19**, 399–442](#)
 1249 <https://doi.org/10.1007/s10498-013-9217-4>, 2013

1250
 1251

1252 Di Biagio V., Cossarini G., Salon S., Lazzari P., Querin S., Sannino G., Solidoro C.: Temporal scales of variability
 1253 in the Mediterranean Sea ecosystem: Insight from a coupled model. *Journal of Marine Systems*.
 1254 <https://doi.org/10.1016/j.jmarsys.2019.05.002>, 2019

1255
 1256 [D’Ortenzio, F., Antoine, D. and Marullo, S.: Satellite-driven modeling of the upper ocean mixed layer and air–sea CO₂](#)
 1257 [flux in the Mediterranean Sea. *Deep Sea Research Part I: Oceanographic Research Papers*, 55\(4\), pp.405-434, 2008](#)

1258
 1259 D’Ortenzio F. and D’Alcala M.R.: On the trophic regimes of the Mediterranean Sea: a satellite analysis. *Biogeosciences*
 1260 6 (2), 139-148, 2009

1261

Diffenbaugh, N. S., Pal, J. S., Giorgi, F., and Gao, X.: Heat stress intensification in the Mediterranean climate change hotspot. *Geophys. Res. Lett.* 34:GL030000. doi: 10.1029/2007GL030000, 2007

~~Dubois, C., Somot, S., Carillo, S. C. A., De'que, M., Dell'Aquila, A. and co-authors: Future projections of the surface heat and water budgets of the Mediterranean Sea in an ensemble of coupled Atmosphere-Ocean Regional Climate Models. *Clim. Dynam.* 39(78), 18591884, 2012~~

Dubois, C., Somot, S., Calmanti, S., Carillo, A., Déqué, M., Dell'Aquila, A., Elizalde, A., Jacob, D., L'Hévéder, B., Li, L., Oddo, P., Sannino, G., Scoccimarro, E., Sevault, F.: Future projections of the surface heat and water budgets of the Mediterranean Sea in an ensemble of coupled atmosphere-ocean regional climate models. *Climate dynamics*, 39(7), 1859-1884., 2012

Fach, B. A., Orek, H., Yilmaz, E., Tezcan, D., Salihoglu, I., Salihoglu, B., and Latif, M. A.: Water Mass Variability and Levantine Intermediate Water Formation in the Eastern Mediterranean Between 2015 and 2017. *Journal of Geophysical Research: Oceans*, 126(2), e2020JC016472., 2021

Fedele, G., Mauri, E., Notarstefano, G., Poulain, P. M.: Characterization of the Atlantic Water and Levantine Intermediate Water in the Mediterranean Sea using Argo Float Data. *Ocean Science Discussions*, 1-41. 2021

Foujols, M.-A., Lévy, M., Aumont, O., Madec, G.: OPA 8.1 Tracer Model Reference Manual. Institut Pierre Simon Laplace, pp. 39., 2000

Gačić, M., Borzelli, G. L. E., Civitarese, G., Cardin, V., Yari, S.(2010).Can internal processes sustain reversals of the ocean upper circulation? The Ionian Sea example.*Geophys. Res. Lett.*, 37, L09608, doi:10.1029/2010GL043216.

Galli, G., Lovato, T., Solidoro, C.: Marine Heat Waves Hazard 3D Maps and the Risk for Low Motility Organisms in a Warming Mediterranean Sea. *Frontiers in Marine Science* 4:136. doi: 10.3389/fmars.2017.00136, 2017

Gazeau, F., Ridame, C., Van Wambeke, F., Alliouane, S., Stolpe, C., Irisson, J.-O., Marro, S., Grisoni, J.-M., De Liège, G., Nunige, S., Djaoudi, K., Pulido-Villena, E., Dinasquet, J., Obernosterer, I., Catala, P., and Guieu, C.: Impact of dust addition on Mediterranean plankton communities under present and future conditions of pH and temperature: an experimental overview, *Biogeosciences*, 18, 5011–5034, <https://doi.org/10.5194/bg-18-5011-2021>, 2021.

Giorgi, F: Climate change hot-spots. *Geophysical research letters*, 33(8).2006

- Giorgi, F., Lionello, P.: Climate Change Projections for the Mediterranean Region. *Glob Planet Change* 63:90-104. doi: 10.1016/j.gloplacha.2007.09.005, 2008
- Goyet, C., Hassoun, A., Gemayel, E., Touratier, F., Abboud-Abi Saab, M. and Guglielmi, V.: Thermodynamic forecasts of the Mediterranean Sea acidification. *Mediterranean Marine Science*, 17(2), pp.508-518., 2016
- Gualdi, S., Somot, S., Li, L., Artale, V., Adani, M., Bellucci, A., [Braun, A., Calmanti, S., Carillo, A., Dell'Aquila, A., Déqué, M., Dubois, C., Elizalde, A., Harzallah, A., Jacob, D., L'Hévéder, B., May, W., Oddo, P., Ruti, P., Sanna, A., Sannino, G., Scoccimarro, E., Sevault, F., Navarra, A et al.](#): The CIRCE simulations: Regional climate change projections with realistic representation of the ~~M~~editerranean sea. *Bulletin of the American Meteorological Society*, 94, 65-81. doi:10.1175/BAMS-D-11-00136.1, 2013
- Guyennon, A., Baklouti, M., Diaz, F., Palmieri, J., Beuvier, J., Lebaupin-Brossier, C., Arsouze, T., Béranger, K., Dutay, J.-C., and Moutin, T.: New insights into the organic carbon export in the Mediterranean Sea from 3-D modeling. *Biogeosciences*, 12, 7025–7046, <https://doi.org/10.5194/bg-12-7025-2015>, 2015.
- Hassoun, A. E. R., Fakhri, M., Abboud-Abi Saab, M., Gemayel, E., and De Carlo, E. H: The carbonate system of the Eastern-most Mediterranean Sea, Levantine Sub-basin: Variations and drivers. *Deep Sea Research Part II: Topical Studies in Oceanography*, 164, 54-73, 2019
- ~~Hausfather, Zeke, Glen P. Peters: "Emissions-the 'business as usual' story is misleading." Nature 577.7792 (2020): 618-620.~~
- Herrmann, M., Somot, S., Sevault, F., Estournel, C., and Déqué, M.: Modeling the deep convection in the northwestern Mediterranean Sea using an eddy-permitting and an eddy-resolving model: Case study of winter 1986–1987, *J. Geophys. Res.*, 113, C04011, doi:10.1029/2006JC003991., 2008
- Herrmann, M., Diaz, F., Estournel, C., Marsaleix, P., Ulses, C.: Impact of atmospheric and oceanic interannual variability on the North~~western~~Western Mediterranean Sea pelagic planktonic ecosystem and associated carbon cycle, *J. Geophys. Res. Oceans*, 118, 5792–5813, doi:10.1002/jgrc.20405., 2013
- Herrmann, M., Estournel, C., Adloff, F., and Diaz, F.: Impact of climate change on the northwestern Mediterranean Sea pelagic planktonic ecosystem and associated carbon cycle, *J. Geophys. Res. Oceans*, 119, 5815– 5836, doi:10.1002/2014JC010016, 2014

- Howes, E.L., Stemmann, L., Assailly, C., Irisson, J.O., Dima, M., Bijma, J., Gattuso, J.P.: Pteropod time series from the North Western Mediterranean (1967-2003): impacts of pH and climate variability. *Mar Ecol Prog Ser* 531:193-206. <https://doi.org/10.3354/meps11322>, 2015
- Ibrahim, O., Mohamed, B., Nagy, H.: Spatial Variability and Trends of Marine Heat Waves in the Eastern Mediterranean Sea over 39 Years. *J. Mar. Sci. Eng.* 9, 643. <https://doi.org/10.3390/jmse9060643>, 2021
- IPCC AR5 Climate Change 2014: Synthesis Report. Contribution of Working Groups I, II and III to the Fifth Assessment Report of the Intergovernmental Panel on Climate Change, 2014
- Keeling, R. F., Kortzinger A., and Gruber N.: Ocean Deoxygenation in a Warming World *Annual Review of Marine Science* 2: 199-229, 2010-
- Kwiatkowski, L., Torres, O., Bopp, L., Aumont, O., Chamberlain, M., Christian, J. R., Dunne, J. P., Gehlen, M., Ilyina, T., John, J. G., Lenton, A., Li, H., Lovenduski, N. S., Orr, J. C., Palmieri, J., Santana-Falcón, Y., Schwinger, J., Séférian, R., Stock, C. A., Tagliabue, A., Takano, Y., Tjiputra, J., Toyama, K., Tsujino, H., Watanabe, M., Yamamoto, A., Yool, A., and Ziehn, T.: Twenty-first century ocean warming, acidification, deoxygenation, and upper-ocean nutrient and primary production decline from CMIP6 model projections, *Biogeosciences*, 17, 3439–3470, <https://doi.org/10.5194/bg-17-3439-2020>, 2020
- Lamon, L., Rizzi, J., Bonaduce, A. et al.: An ensemble of models for identifying climate change scenarios in the Gulf of Gabes, Tunisia *Reg Environ Change* 31. <https://doi.org/10.1007/s10113-013-0430-x>, 2014
- ~~Lascaratos, A.: Estimation of deep and intermediate water mass formation rates in the Mediterranean Sea. *Deep Sea Research II*, 40, 1327–1332, 1993-~~
- Lazzari, P., Solidoro, C., Ibello, V., Salon, S., Teruzzi, A., Béranger, K., Colella, S., Crise, A.: Seasonal and inter-annual variability of plankton chlorophyll and primary production in the Mediterranean Sea: a modelling approach, *Biogeosciences*, 9, 217-233, doi:10.5194/bg-9-217-2012, 2012
- Lazzari, P., G-Mattia, G., C-Solidoro, C., S-Salon, S., A-Crise, A., M-Zavatarelli, M., P-Oddo, P., M-Vichi M.: The impacts of climate change and environmental management policies on the trophic regimes in the Mediterranean Sea: Scenario analyses *Journal of Marine Systems* Sea, 2014
- Lazzari, P., Solidoro C., Salon S., Bolzon G.: Spatial variability of phosphate and nitrate in the Mediterranean Sea: A modeling approach *Deep Sea Research* Pages 39-52, 2016

- Lavigne, H., D'Oertenzio, F., De'Alcalà, M. R., Claustre, H., Sauzede, R., and Gacic, M.: On the vertical distribution of the chlorophyll a concentration in the Mediterranean Sea: a basin-scale and seasonal approach. *Biogeosciences*, 12(16), 5021-5039, 2015
- Lionello, P., Abrantes, F., Congedi, L., Dulac, F., Gacic, M., Gomis, D., Goodess, C., Hoff, H., Kutiel, H., Luterbacher, J., Planton, S., Reale, M., Schröder, K., Struglia, M. V., Toreti, A., Tsimplis, M., Ulbrich, U., Xoplaki, E.: Introduction: Mediterranean Climate: Background Information in Lionello P. (Ed.) *The Climate of the Mediterranean Region. From the Past to the Future*, Amsterdam: Elsevier (NETHERLANDS), XXXV-1XXX, ISBN:9780124160422, 2012
- Lovato, T., Vichi, M., Oddo, P.: High-resolution simulations of Mediterranean Sea physical oceanography under current and scenario climate conditions: model description, assessment and scenario analysis. *CMCC Research Paper*, RP0207.2013, 2013
- Macias, D., Stips, A., and Garcia-Gorritz, E.: The relevance of deep chlorophyll maximum in the open Mediterranean Sea evaluated through 3D hydrodynamic-biogeochemical coupled simulations. *Ecological Modelling*, 281, 26-37, 2014
- Macias, D. M., Garcia-Gorritz, E., and Stips, A.: Productivity changes in the Mediterranean Sea for the twenty-first century in response to changes in the regional atmospheric forcing. *Frontiers in Marine Science*, 2, 79, 2015.
- Macias D., Garcia-Gorritz E., Stips A.: Deep winter convection and phytoplankton dynamics in the NW Mediterranean Sea under present climate and future (horizon 2030) scenarios. *Sci. Rep.* 22, 1–15. <https://doi.org/10.1038/s41598-018-24965-0>, 2018
- Madec, G.: NEMO Ocean Engine. Note du Pôle de modélisation, No 27, Institut Pierre-Simon Laplace (IPSL), France, 2008
- Mantziafou, A. and Lascaratos, A.: An eddy resolving numerical study of the general circulation and deep-water formation in the Adriatic Sea, *Deep Sea Res., Part I*, 51(7), 251–292., 2004
- Mantziafou, A. and Lascaratos, A.: Deep-water formation in the Adriatic Sea: Interannual simulations for the years 1979-1999, *Deep Sea Res., Part I*, 55, 1403–1427, 2008
- Mathbout, S., Lopez-Bustins, J.A., Royé, D., Martin-Vide, J.: Mediterranean-Scale Drought: Regional Datasets for Exceptional Meteorological Drought Events during 1975–2019. *Atmosphere*, 12, 941. <https://doi.org/10.3390/atmos12080941>, 2021

[MedECC \(2020\) Climate and Environmental Change in the Mediterranean Basin – Current Situation and Risks for the Future. First Mediterranean Assessment Report \[Cramer, W., Guiot, J., Marini, K. \(eds.\)\] Union for the Mediterranean, Plan Bleu, UNEP/MAP, Marseille, France, 632pp., ISBN: 978-2-9577416-0-1, DOI: 10.5281/zenodo.4768833, 2020](#)

~~[MedECC Climate and Environmental Change in the Mediterranean Basin: Current Situation and Risks for the Future. First Mediterranean Assessment Report \[Cramer, W., Guiot, J., Marini, K. \(eds.\)\] Union for the Mediterranean, Plan Bleu, UNEP/MAP, Marseille, France, 600pp, 2020](#)~~

Myers, PG and Haines, K: Stability of the Mediterranean's thermohaline circulation under modified surface evaporative fluxes. *J Geophys Res* 107(C3):7-1-10, 2002

Morel, A. and Gentili, B.: The dissolved yellow substance and the shades of blue in the Mediterranean Sea, *Biogeosciences*, 6, 2625–2636, <https://doi.org/10.5194/bg-6-2625-2009>, 2009

Moullec, F., Barrier, N., Drira, S., Guilhaumon, F., Marsaleix, P., Somot, S., ~~Ulises, C., Velez, L., ...~~ and Shin, Y. J.: An end-to-end model reveals losers and winners in a warming Mediterranean Sea. *Frontiers in Marine Science*, 6, 345. 2019

Moutin, T. and Raimbault, P.: Primary production, carbon export and nutrients availability in ~~western~~[Western](#) and ~~eastern~~[Eastern](#) Mediterranean Sea in early summer 1996 (MINOS cruise), *J. Marine Syst.*, 33/34, 273–288, 2002

~~[Moutin, T. and Prieur, L.: Influence of anticyclonic eddies on the Biogeochemistry from the Oligotrophic to the Ultraoligotrophic Mediterranean \(BOUM cruise\), *Biogeosciences*, 9, 3827–3855, <https://doi.org/10.5194/bg-9-3827-2012>, 2012.](#)~~

Moss, R. H., Edmonds, J. A., Hibbard, K. A., Manning, M. R., Rose, S. K., Van Vuuren, D. P., Meehl, G. A.: The next generation of scenarios for climate change research and assessment. *Nature*, 463(7282), 747-756, 2010

~~[Nittis K. and Lascaratos A.: Diagnostic and prognostic numerical studies of LIW formation. *Journal of Marine Systems*, 18, 179–195, 1998](#)~~

O'Connor, M. I., Gilbert, B., and Brown, C. J.: Theoretical predictions for how temperature affects the dynamics of interacting herbivores and plants. *The American Naturalist*, 178(5), 626-638, 2011

~~[O'Neill, B. C., Tebaldi, C., Vuuren, D. P. V., Eyring, V., Friedlingstein, P., Hurtt, G., ... and Sanderson, B. M.: The scenario model intercomparison project \(ScenarioMIP\) for CMIP6. *Geoscientific Model Development*, 9\(9\), 3461-3482. 2016](#)~~

- O'Neill, B. C., Tebaldi, C., van Vuuren, D. P., Eyring, V., Friedlingstein, P., Hurtt, G., Knutti, R., Kriegler, E., Lamarque, J.-F., Lowe, J., Meehl, G. A., Moss, R., Riahi, K., and Sanderson, B. M.: The Scenario Model Intercomparison Project (ScenarioMIP) for CMIP6, *Geosci. Model Dev.*, 9, 3461–3482, <https://doi.org/10.5194/gmd-9-3461-2016>, 2016.
- Oddo, P., Adani, M., Pinardi, N., Fratianni, C., Tonani, M., and Pettenuzzo, D.: A nested Atlantic-Mediterranean Sea general circulation model for operational forecasting. *Ocean Science*, 5, 461–473. <https://doi.org/10.5194/os-5-461-2009>, 2009
- Pagès R., Baklouti, M., Barrier, N., Ayache, M., Sevault, F., Somot, S., and Moutin, T.: Projected Effects of Climate-Induced Changes in Hydrodynamics on the Biogeochemistry of the Mediterranean Sea Under the RCP 8.5 Regional Climate Scenario. *Frontiers in Marine Science*, 7, 957, 2020
- Planton, S., ~~P.~~Lionello, ~~P.~~~~V.~~Artale,~~V.~~~~R.~~Aznar, ~~R.~~~~A.~~Carrillo, ~~A.~~~~J.~~Colin,~~J.~~~~L.~~Congedi, ~~L.~~~~C.~~Dubois, ~~C.~~~~A.~~Elizalde, ~~A.~~~~S.~~Gualdi, ~~S.~~~~E.~~Hertig, ~~E.~~~~J.~~Jacobeit, ~~J.~~~~G.~~Jordà, ~~G.~~~~L.~~Li, ~~L.~~~~A.~~Mariotti, ~~A.~~~~C.~~Piani, ~~C.~~~~P.~~Ruti,~~P.~~~~E.~~Sanchez-Gomez, ~~E.~~~~G.~~Sannino, ~~G.~~~~F.~~Sevault, ~~F.~~~~S.~~Somot, ~~S.~~~~M.~~Tsimplis:~~M.~~—The Climate of the Mediterranean Region in Future Climate in Lionello P. (Ed.) *The Climate of the Mediterranean Region. From the Past to the Future*-, Amsterdam: Elsevier (NETHERLANDS), Projections 449-502, 2012
- Powley, H. R., Krom, M. D., and Van Cappellen, P.: Circulation and oxygen cycling in the Mediterranean Sea: Sensitivity to future climate change, *J. Geophys. Res. Oceans*, 121, 8230–8247, doi:10.1002/2016JC012224, 2016
- Ramirez-Romero, E., Jordà, G., Amores, A., Kay, S., Segura-Noguera, M., Macias, DM., Maynou, F., Sabatés, A. and Catalán, IA.: Assessment of the Skill of Coupled Physical–Biogeochemical Models in the NW Mediterranean. *Front. Mar. Sci.* 7:497. doi: 10.3389/fmars.2020.00497, 2020
- Reale, M., Giorgi, F., Solidoro, C., Di Biagio, V., Di Sante, F., Mariotti, L., Farneti, R., Sannino, G.: The Regional Earth System Model RegCM-ES: Evaluation of the Mediterranean climate and marine biogeochemistry. *Journal of Advances in Modeling Earth Systems*, 12, e2019MS001812. <https://doi.org/10.1029/2019MS001812>, 2020a
- Reale, M., Salon, S., Somot, S., Solidoro, C., Giorgi, F., Cossarini, G., Lazzari, P., Crise, A., Sevault, F.: Influence of large-scale atmospheric circulation patterns on nutrients dynamics in the Mediterranean Sea in the extended winter season (October–March) 1961–1999 *Climate Research* <https://doi.org/10.3354/cr01620>, 2020b
- Richon, C., Dutay, J.-C., Dulac, F., Wang, R., Balkanski, Y.: Modeling the biogeochemical impact of atmospheric phosphate deposition from desert dust and combustion sources to the Mediterranean Sea, *Biogeosciences*, 15, 2499–2524, <https://doi.org/10.5194/bg-15-2499-2018>, 2018

- Richon, C., Dutay, J.-C., Bopp, L., Le Vu, B., Orr, J. C., Somot, S., Dulac, F.: Biogeochemical response of the Mediterranean Sea to the transient SRES-A2 climate change scenario, *Biogeosciences*, 16, 135-165, <https://doi.org/10.5194/bg-16-135-2019>, 2019
- Salon, S., Cossarini, G., Bolzon, G., Feudale, L., Lazzari, P., Teruzzi, A., Solidoro, C., and Crise, A.: Novel metrics based on Biogeochemical Argo data to improve the model uncertainty evaluation of the CMEMS Mediterranean marine ecosystem forecasts, *Ocean Sci.*, 15, 997–1022, <https://doi.org/10.5194/os-15-997-2019>, 2019
- Schroeder, K., Garcia-Lafuente, J., Josey, S.A., Artale, V., Nardelli, B.B., Carrillo, A., Gačić, M., Gasparini, G.P., Herrmann, M., Lionello, P., Ludwig, W., Millot, C., Özsoy, E., Pisacane, G., Sánchez-Garrido, J.C., Sannino, G., Santoleri, R., Somot, S., Struglia, M., Stanev, E., Taupier-Letage, I., Tsimplis, M.N., Vargas-Yáñez, M., Zervakis, V., Zodiatis, G.: Circulation of the Mediterranean Sea and its Variability. in P. Lionello (ed.), *The Climate of the Mediterranean Region: From the Past to the Future*. Elsevier Inc., pp. 187-256. <https://doi.org/10.1016/B978-0-12-416042-2.00003-3>, 2012
- Scoccimarro, E., ~~S.~~ Gualdi, ~~S.~~ A. Bellucci, ~~A.~~ A. Sanna, ~~A.~~ P. G. Fogli, ~~P. G.~~ E. Manzini, ~~E.~~ M. Vichi, ~~M.~~ P. Oddo, ~~P.~~ and ~~A.~~ Navarra, ~~A.~~: Effects of Tropical Cyclones on Ocean Heat Transport in a High Resolution Coupled General Circulation Model. *Journal of Climate*, 24, 4368-4384, 2011
- [Shepherd, J. G., Brewer, P. G., Oschlies, A., & Watson, A. J.: Ocean ventilation and deoxygenation in a warming world: introduction and overview. *Philosophical Transactions of the Royal Society A: Mathematical, Physical and Engineering Sciences*, 375\(2102\), 20170240, 2017](https://doi.org/10.1093/gi/fgz001)
- Simoncelli, S., Fratianni, C., Pinardi, N., Grandi, A., Drudi, M., Oddo, P., and Dobricic, S.: Mediterranean Sea Physical Reanalysis (CMEMS MED-Physics) [Data set]. Copernicus Monitoring Environment Marine Service (CMEMS). https://doi.org/10.25423/MEDSEA_REANALYSIS_PHYS_006_004, 2019
- Siokou-Frangou, I., Christaki, U., Mazzocchi, M., Montresor, M., Ribera d'Alcala, M., Vaque, D., Zingone, A.: Plankton in the open Mediterranean sea: a review. *Biogeosciences*, 7(5):1543-1586., 2010
- Sitz, L. E., ~~D.~~ di Sante, F., Farneti, R., Fuentes-Franco, R., Coppola, E., Mariotti, L., Reale, M., Sannino, G., Barreiro, M., Nogherotto, R., Giuliani, G., Graffino, G., Solidoro, C., Cossarini, G., and Giorgi, F.: Description and evaluation of the Earth System Regional Climate Model (Reg CM-ES). *Journal of Advances in Modeling Earth Systems*, 9, 1863–1886. <https://doi.org/10.1002/2017MS000933>, 2017
- Solidoro, C., Cossarini, G., Lazzari, P., Galli, G., Bolzon, G., Somot, S., Sevault, F., Salon, S.: Modelling carbon budgets in the Mediterranean Sea ecosystem under contemporary and future climate. Submitted to *Frontiers in Marine Sciences*, 2022[†]

1517

1518 Somot₂ S., Sevault₂ F., Déqué₂ M.: Transient climate change scenario simulation of the Mediterranean Sea for the 21st
1519 century using a high-resolution ocean circulation model. *Climate Dynamics*, Springer Verlag, 27 (7-8), pp.851-879.
1520 [ff10.1007/s00382-006-0167-z](https://doi.org/10.1007/s00382-006-0167-z)ff. [ffhal-00195045f](https://doi.org/10.1007/s00382-006-0167-z), 2006

1521

1522 Somot₂ S., Houpert₂ L., Sevault₂ F., Testor₂ P., Bosse₂ A., Taupier-Letage₂ I., Bouin₂ M., Waldman₂ R., Cassou₂ C.,
1523 Sanchez-Gomez₂ E., Durrieu de Madron₂ X., Adloff₂ F., Nabat₂ P., Herrmann, M.: Characterizing, modelling and
1524 understanding the climate variability of the deep water formation in the North-~~Western~~^{Western} Mediterranean Sea.
1525 *Climate Dynamics* 51, 1179–1210. <https://doi.org/10.1007/s00382-016-3295-0>, 2018

1526

1527 Soto-Navarro, J., Jordá, G., Amores, A., ~~Cabos, W., Somot, S., Sevault, F., Macias, D., Djurdjevic V., Sannino G., Li~~
1528 ~~L., Sein D.et al.~~: Evolution of Mediterranean Sea water properties under climate change scenarios in the Med-CORDEX
1529 ensemble, *Clim Dyn* 54, 2135–2165. <https://doi.org/10.1007/s00382-019-05105-4>, 2020

1530

1531 [Stöven, T. and Tanhua, T.: Ventilation of the Mediterranean Sea constrained by multiple transient tracer measurements,](https://doi.org/10.5194/os-10-439-2014)
1532 [Ocean Sci., 10, 439–457, https://doi.org/10.5194/os-10-439-2014, 2014.](https://doi.org/10.5194/os-10-439-2014)

1533

1534

1535 Taylor, K. E., Stouffer, R. J., and Meehl, G. A.: An Overview of CMIP5 and the Experiment Design, *B. Am. Meteorol.*
1536 *Soc.*, 93, 485–498, <https://doi.org/10.1175/BAMS-D-11-00094.1>, 2012.

1537

1538 Teruzzi₂ A., Dobricic₂ S., Solidoro₂ C., Cossarini₂ G.: A 3D variational assimilation scheme in coupled transport
1539 biogeochemical models: Forecast of Mediterranean biogeochemical properties, *Journal of Geophysical Research*,
1540 [doi:10.1002/2013JC009277](https://doi.org/10.1002/2013JC009277), 2014

1541

1542 Teruzzi₂ A., Bolzon₂ G., Salon₂ S., Lazzari₂ P., Solidoro₂ C., Cossarini₂ G.: Assimilation of coastal and open sea
1543 biogeochemical data to improve phytoplankton simulation in the Mediterranean Sea. *Ocean Modelling*,
1544 <https://doi.org/10.1016/j.ocemod.2018.09.007>2018, 2018

1545

1546 Teruzzi, A., Bolzon, G., Cossarini, G., Lazzari, P., Salon, S., Crise, A., and Solidoro, C.: Mediterranean Sea
1547 Biogeochemical Reanalysis (CMEMS MED-Biogeochemistry) [Data set]. Copernicus Monitoring Environment Marine
1548 Service (CMEMS). https://doi.org/10.25423/MEDSEA_REANALYSIS_BIO_006_008, 2019

1549

1550 Teruzzi, A., ~~Di Biagio, V.~~, Feudale, L., Bolzon, G., Lazzari, P., Salon, S., Di Biagio, V., Coidessa, G., and Cossarini, G.:
1551 Mediterranean Sea Biogeochemical Reanalysis (CMEMS MED-Biogeochemistry, MedBFM3 system) (Version 1) [Data
1552 set]. Copernicus Monitoring Environment Marine Service (CMEMS).
1553 https://doi.org/10.25423/CMCC/MEDSEA_MULTIYEAR_BGC_006_008_MEDBFM3, 2021

1554

- Thingstad, T. F., Krom, MD, Mantoura, RF, Flaten, GA, Groom, S, Herut, B, Kress, N, Law, CS, Pasternak, A, Pitta, P, Psarra, S, Rassoulzadegan, F, Tanaka, T, Tselepides, A, Wassmann, P, Woodward, EM, Riser, CW, Zodiatis, G, Zohary, T, ~~rede, et al.~~: Nature of phosphorus limitation in the ultraoligotrophic ~~eastern~~Eastern Mediterranean. *Science* 309.5737: 1068-1071, 2005
- Van Apeldoorn, D. and Bouwman, L.: SES land-based runoff and nutrient load data (1980-2000), Deliverable 4.6, http://www.perseus-net.eu/assets/media/PDF/deliverables/3321.6_Final.pdf, last access 05-02-2020, 2014
- [Velaoras, D., Papadopoulos, V. P., Kontoyiannis, H., Cardin, V., & Civitarese, G. : . Water masses and hydrography during April and June 2016 in the cretan sea and cretan passage \(Eastern Mediterranean Sea\). *Deep Sea Research Part II: Topical Studies in Oceanography*, 164, 25-40, 2019](#)
- Vichi, M., Allen, J. I., Masina, S., and Hardman-Mountford, N. J.: The emergence of ocean biogeochemical provinces: A quantitative assessment and a diagnostic for model evaluation, *Global Biogeochem. Cycles*, 25, GB2005, doi:10.1029/2010GB003867, 2011
- Vichi, M., Cossarini, G., Gutierrez Mlot E., Lazzari P., Lovato T., Mattia G., Masina S., McKiver W., Pinardi N., Solidoro C., Zavatarelli M., The Biogeochemical Flux Model (BFM): Equation Description and User Manual. BFM version 5 (BFM-V5). Release 1.0, BFM Report series N, 1. March 2013. CMCC, Bologna, Italy, <http://bfm-community.eu>, p. 87, 2015
- Waldman, R., Brüggemann, N., Bosse, A., Spall, M., Somot, S., and Sevault, F.: Overturning the Mediterranean thermohaline circulation. *Geophysical Research Letters*, 45, 8407– 8415. <https://doi.org/10.1029/2018GL078502>, 2018
- [Wimart-Rousseau, C., Lajaunie-Salla, K., Marrec, P., Wagener, T., Raimbault, P., Lagadec, V., Lafont, M., Garcia, N., Diaz, F., Pinazo, C., Yohia, C., Garcia, F., Xueref-Remy, I., Blanc, P., Armengaud, A., and Lefèvre, D.: Temporal variability of the carbonate system and air-sea CO₂ exchanges in a Mediterranean human-impacted coastal site. *Estuarine, Coastal and Shelf Science*, 236, 106641, 2020](#)
- Wolf-Gladrow, D. A., Zeebe, R. E., Klaas, C., Körtzinger, A., and Dickson, A. G: Total alkalinity, the explicit conservative expression and its application to biogeochemical processes. *Marine Chemistry*, 106(1), 287-300, 2007
- Zunino, S., Canu, D. M., Bandelj, V., and Solidoro, C.: Effects of ocean acidification on benthic organisms in the Mediterranean Sea under realistic climatic scenarios: a meta-analysis. *Regional Studies in Marine Science*, 10, 86-96., 2017

1593 Zunino, S., Canu, D. M., Zupo, V., and Solidoro, C.: Direct and indirect impacts of marine acidification on the ecosystem
1594 services provided by coralligenous reefs and seagrass systems. *Global Ecology and Conservation*, 18, e00625, 2019
1595
1596 Zunino, S., Libralato, S., Melaku Canu, D., Prato G. and Solidoro C.: Impact of Ocean Acidification on Ecosystem
1597 Functioning and Services in Habitat-Forming Species and Marine Ecosystems. *Ecosystems*
1598 <https://doi.org/10.1007/s10021-021-00601-3>, 2021
1599